Journal of Medicinal Chemistry

pubs.acs.org/jmc

Drug Annotation

Discovery of EST73502, a Dual μ-Opioid Receptor Agonist and σ_1 Receptor Antagonist Clinical Candidate for the Treatment of Pain

Mónica García, Marina Virgili, Mònica Alonso, Carles Alegret, Joan Farran, Begoña Fernández, Magda Bordas, Rosalia Pascual, Javier Burgueño, Alba Vidal-Torres, Antonio R. Fernández de Henestrosa, Eva Ayet, Manuel Merlos, Jose Miguel Vela, Carlos R. Plata-Salamán, and Carmen Almansa*

Cite This: https://dx.doi.org/10.1021/acs.jmedchem.0c01127

Read Online

ACCESS | Metrics & More | Article Recommendations | Supporting Information

ABSTRACT: The synthesis and pharmacological activity of a new series of 4-alkyl-1-oxa-4,9-diazaspiro[5.5]undecane derivatives as potent dual ligands for the σ_1 receptor (σ_1R) and the μ-opioid receptor (MOR) are reported. A lead optimization program over the initial 4-aryl analogues provided 4-alkyl derivatives with the desired functionality and good selectivity and ADME profiles. Compound **14u** (EST73502) showed MOR agonism and σ_1R antagonism and a potent analgesic activity, comparable to the MOR agonist oxycodone in animal models of acute and chronic pain after single and repeated administration. Contrary to oxycodone, **14u** produces analgesic activity with reduced opioid-induced relevant adverse events, like intestinal transit inhibition and naloxone-precipitated behavioral signs of opiate withdrawal. These results provide evidence that dual MOR agonism and σ_1R antagonism may be a useful strategy for obtaining potent and safer analgesics and were the basis for the selection of **14u** as a clinical candidate for the treatment of pain.

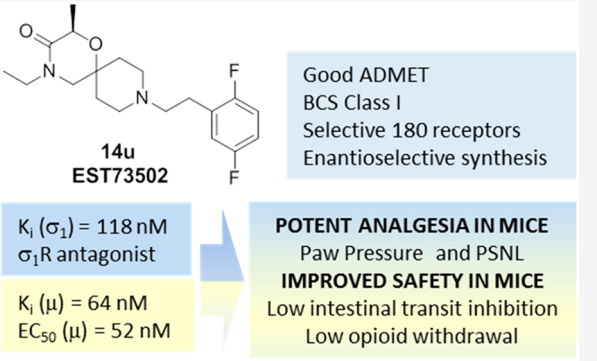

INTRODUCTION

Currently available pain therapies are often suboptimal in terms of efficacy and side effects,[1] with a high percentage of population remaining undertreated. As a new strategy to address this high unmet medical need, we recently reported the development of dual compounds targeting both the μ-opioid receptor (MOR) and the σ_1 receptor (σ_1R).[2] MOR agonists, represented here by oxycodone (**1**, Figure 1), are recognized as the most effective therapies when addressing severe pain states, but their administration is limited by their important side effects, such as constipation, respiratory depression, emesis, and physical dependence.[3] In addition, after long-term use MOR agonists can induce the development of analgesic tolerance that leads to substantial increases in dosing in order to maintain a clinically satisfactory pain relief. This is partially explained at the molecular level by a MOR down-regulation,[4] although other phenomena may be involved. Taking into account the narrow therapeutic window of MOR agonists, this tolerance finally results in unacceptable side effects, poor patient compliance, and addiction, as revealed by the recent opioid crisis affecting the USA.[5]

The rationale behind the strategy of targeting in the same compound the MOR and the σ_1 receptor (σ_1R) is linked to both the role of the σ_1R in central sensitization, which could add value to types of pain where the opioids are less effective,

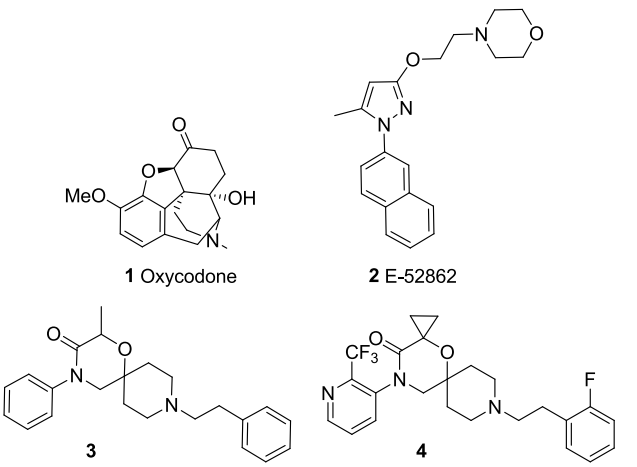

Figure 1. Structures of oxycodone (**1**, MOR agonist), E-52862 (**2**, σ_1R antagonist), and dual MOR and σ_1R ligands **3** and **4**.

Received: July 1, 2020

Scheme 1[a]

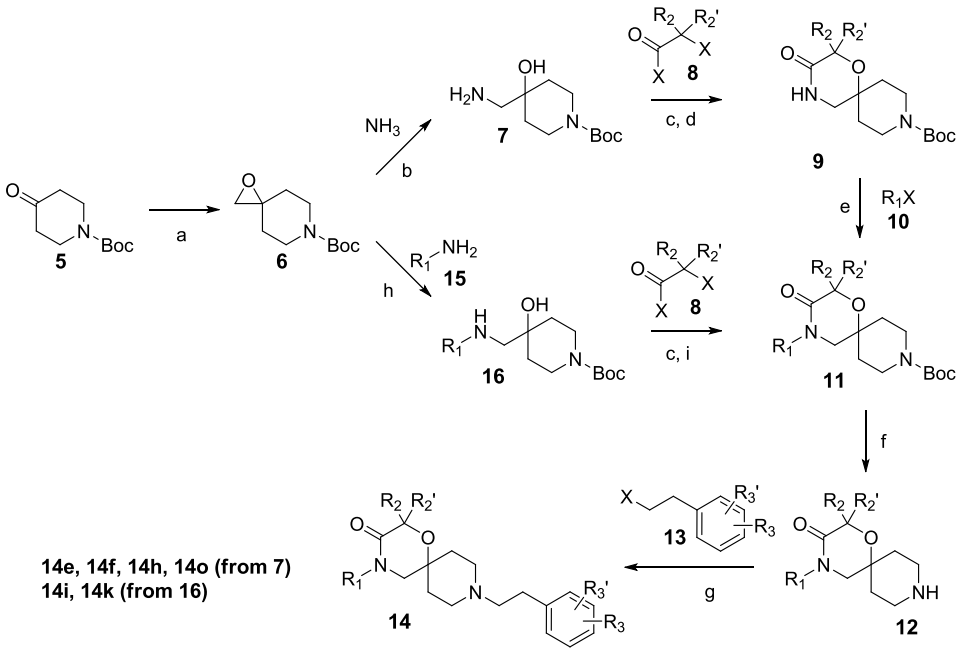

[a]Reagents and conditions: (a) TMSOI, ^{t}BuOK, DMSO−DME, 0−5 °C, 1 h; (b) MeOH, rt, 16 h; (c) K_2CO_3, EtOAc−water, 0 °C, 30 min, or TEA, DCM, 0 °C; (d) ^{t}BuOK, THF, rt, 16 h; (e) NaH, DMF, rt; (f) TFA, DCM, rt or reflux; (g) K_2CO_3 or DIPEA, NaI, acetonitrile, 80 °C, 16 h; (h) EtOH−water 9:1, rt, 16 h; (i) ^{t}BuOK, THF, −78 to −30 °C, 1−4 h.

and its potentiation of opioid analgesia. In fact, the σ_1R was first described as an endogenous anti-opioid system, based on the finding that σ_1R agonists counteracted MOR mediated analgesia, while σ_1R antagonists potentiated it.[6] Later on, the involvement of the σ_1R in pain was confirmed both by the development of the σ_1R knockout mice (σ_1R-KO),[7] which show no obvious phenotype and perceive normally sensory stimuli, and by the discovery of σ_1R antagonists, such as S1RA (E-52862, **2**).[8] Some of the findings observed with compound **2** support the potential therapeutic value of a dual MOR agonist/σ_1R antagonist for the treatment of pain. In rodents S1RA administered in combination with morphine potentiated its analgesia but not its adverse effects,[9] and these findings were reproduced with other σ_1R and MOR ligands and different kinds of pain models.[10] In the clinic, S1RA was associated with a relevant reduction of opioid-associated adverse events (nausea, vomiting, and dizziness) and a meaningful reduction for the need of concomitant antiemetic medication.[11]

Compared to the standard clinical practice of using cocktails or multicomponent drugs, developing dual agents offers the advantages of a broader spectrum of action, better treatment compliance, lowering the risk of drug−drug interactions, simpler pharmacokinetics, and less variability among patients.[12] However, combining two mechanisms of action in a single molecule, while keeping at the same time selectivity for other targets, is a major challenge from the medicinal chemistry point of view.[13] In particular, combining in the same molecule a MOR agonist and σ_1R antagonist profile represented an additional particular issue, since although the assessment of functionality over the MOR receptor is well established, there is no high throughput test for establishing the functionality of σ_1R ligands, often characterized only after in vivo testing.[14] Additionally, getting the good ADME and physicochemical properties required for in vivo activity is more complex than when addressing one single target, since often the dual activity is achieved by combining (i.e., adding) two pharmacophores and it is well-known that large, lipophilic, and flexible molecules are often associated with bad in vivo efficacy and toxicological profiles.[13] These problems were avoided using a pharmacophore merging approach (i.e., combining the two target pharmacophores in the same central core), which led to the development of the 4-aryl-1-oxa-4,9-diazaspiro[5.5]-undecane derivatives represented by the parent compound **3**[2] (Figure 1). The structure−activity relationships (SARs) around **3** showed that either changing the phenethyl group to benzyl or alkyl groups or reducing the size of any of the six-membered rings of the central scaffold to five-membered rings provided a loss of MOR affinity. In addition, the series showed poor selectivity versus the α_1A adrenoreceptor (α_1AR) and the human ether-a-go-go-related gene (hERG), the well-known potassium channel linked to cardiac toxicity.[15] This initial SAR study maintained an aryl group in position 4 and provided lead compound **4**, which showed improved hERG inhibition but still retained some α_1AR affinity and had lost some MOR activity in relation to **3**. The desired ratio of in vitro affinities for the dual compounds is complex to establish, but a predominant affinity for MOR would not make evident the enhancement of the opioid analgesia provided by the σ_1R antagonist component. Note that σ_1R antagonists are inactive when administered alone in acute nociceptive tests[9,16] but induce a leftward shift of the dose−response curve of opioids (including partial and weak MOR agonists) vs the curve obtained with the same opioids given alone, thus suggesting an enhancement of the opioid potency.[9] However, such a potentiating effect was obtained with doses of opioids producing low to moderate activity when given alone and which are lower than those of σ_1R ligands (for example, morphine at 2.5−5 mg/kg and σ_1R antagonist **2** at 40 mg/kg) and maximal enhancement occurs when opioids are combined

https://dx.doi.org/10.1021/acs.jmedchem.0c01127
J. Med. Chem. XXXX, XXX, XXX−XXX

Table 1. Exploration of Substituents in R_1

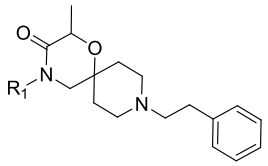

compd	R_1	K_i MOR[a] (*h*, nM)	EC_{50} MOR[b] (*h*, nM)	E_{max} MOR[c] (%)	K_i σ_1R[d] (*h*, nM)	cLogP	hERG[e] IC_{50} (μM)	α_1AR[f] % inh (1 μM)	M[g]
1		12 ± 3	17 ± 9	100	>10000[h]	0	>10[h]		
2		>10000[h]	>10000[h]		17 ± 7	3.9	>10[h]		
3		7 ± 6	14 ± 2	85	6 ± 0.4	4.2	0.4	72	
4		175 ± 85	195 ± 19	100	58 ± 10	3.8	>10[h]	57	
14a	benzyl	2 ± 0.3	2 ± 0.1	97	10 ± 3	3.9	0.1	67	2
14b	2-phenylethyl	20 ± 2	22 ± 13	94	12 ± 2	4.3	0.2	58	2
14c	cyclopropyl[i]	6 ± 1	7 ± 1	91	58 ± 15	2.7	4.5	51	4
14d	isopropyl	33 ± 5	21 ± 2	100	30 ± 5	3.2	3.9	35	2
14e	ethyl	41 ± 12	65 ± 4	84	43 ± 5	2.9	3.1	27	1
14f	methyl	156 ± 5	787 ± 162	79	142 ± 28	2.2	>10[h]	16	1
17	H[j]	>1000[k]	>1000[k]		892 ± 196	1.8	>10[h]	7	1

[a]Binding affinity (K_i) in a MOR binding assay using [^{3}H]-DAMGO as radioligand. Each value is the mean ± SD of at least two determinations. [b]MOR functionality (EC_{50}) measuring cyclic AMP (cAMP) on CHO-K1 cells. Each value is the mean ± SD of two determinations. [c]Efficacy of 100% is defined as the maximum effect induced by stimulation with DAMGO. It is provided for compounds showing EC_{50} below 1000 nM in the functional assay. [d]Binding affinity (K_i) to human σ_1R in transfected HEK-293 membranes using [^{3}H](+)-pentazocine as radioligand. Each value is the mean ± SD of two determinations. [e]Whole-cell patch clamp hERG blockade. [f]Percentage inhibition of α1A receptor at 1 μM ligand concentration. [g]Methods used for the synthesis of compounds according to the schemes described in the Chemistry section. [h]Less than 50% inhibition at 10 μM. [i]Enantiopure compound (*R* stereochemistry). [j]2-Fluorophenethyl in piperidine. [k]Less than 50% inhibition at 1 μM.

at low doses (around their ED_{25} if administered alone).[9] In addition, it is known that pharmacological σ_1R antagonism enhances opioid antinociception but not opioid-related adverse effects.[9] Thus, the maximum benefit-to-risk ratio is expected for a drug combining σ_1R antagonism with weak/partial MOR agonism (efficacy would result from σ_1R antagonism-mediated maximization of modest opioid effect, whereas side effects would rely on such nonpotentiated baseline opioid component).

We report here the lead optimization program over **4**, which led to the identification of the dual MOR agonist and σ_1R antagonist, (*R*)-9-(2,5-difluorophenethyl)-4-ethyl-2-methyl-1-oxa-4,9-diazaspiro[5.5]undecan-3-one (EST73502, **14u**), as a clinical candidate for the treatment of pain.

CHEMISTRY

The synthesis of the compounds described herein[17] was accomplished as described in Schemes 1−4 and indicated in Tables 1−4. Following a similar strategy to that described in our previous paper for R_1 = aryl analogues,[2] a highly versatile route was devised to prepare derivatives **14**, allowing diversification in substituents R_1−R_3 (Scheme 1). Starting from the *N*-Boc-piperidone **5**, epoxide **6** was prepared[18] using Corey−Chaykovsky reagent[19] with potassium *tert*-butoxide as the base. Next, ring opening with methanolic ammonia led to aminoalcohol **7** in good yield. Acylation with an adequate acyl halide **8** (see experimental part for the preparation of 2-bromo-4-chlorobutanoyl chloride[20]) and final intramolecular cyclization in the presence of potassium *tert*-butoxide at room temperature rendered spirocyclic compounds **9** that were N-alkylated to obtain key intermediates **11**. Alternatively, compounds **11** were also prepared by direct ring-opening of epoxide **6** with alkylamines **15** to afford amino alcohols **16**. In this case, after acylation with **8**, final cyclization with potassium *tert*-butoxide was best performed at low temperatures. Finally, Boc-deprotection followed by N-alkylation with phenethyl derivatives **13** provided the target compounds **14** in good yields.

Compound **17** (Table 1) was prepared from compound **9-1** (where R_2 = Me, $R_{2'}$ = H) by direct Boc-deprotection followed by N-alkylation with 2-fluorophenethyl bromide as described above for the preparation of compounds **14** from **11**.

Although Scheme 1 is of general application, some variations were used in particular cases. *N*-Phenethylpiperidone **18** is commercially available and was used to prepare compounds **14** bearing the phenethyl substituent right from the start (Scheme 2). A strategy similar to that described in Scheme 1 afforded in good yield key intermediate **21**, which was N-alkylated to render target compounds **14a,b,d**.

An even shorter route was used to prepare compounds **14g**, **14l**, and **14m**, by opening of the epoxide **19** with methylamine, followed by acylation and cyclization (Scheme 3). Dimethylated compound **14m** was best prepared using longer reaction times and higher temperatures in both steps. Chiral compound **14g** was obtained with ee 90−93% using chiral (*S*)-2-chloropropanoyl chloride **8-1S** as the acylating agent in a biphasic system (EtOAc−water) and assuming inversion of configuration in the cyclization step; final enrichment via crystallization of the hydrochloride salt was performed to reach ee >98% (as determined by chiral HPLC).

Enantiopure compounds were more conveniently synthesized using the optimized procedure shown in Scheme 4 and detailed for compound **14u** (described in the Experimental Section as representative example). Acylation of amino alcohols **16** with enantiopure acyl chlorides **8S**, followed by treatment with potassium *tert*-butoxide and assuming inversion of configuration in the cyclization, provided key intermediates **11** as the *R*-enantiomer (**11R**) with excellent yield and ee 90−94% as determined by chiral HPLC. Crystallization from a suitable solvent (i.e., for **11-1R** a mixture of isopropyl acetate

https://dx.doi.org/10.1021/acs.jmedchem.0c01127
J. Med. Chem. XXXX, XXX, XXX−XXX

Scheme 2[a]

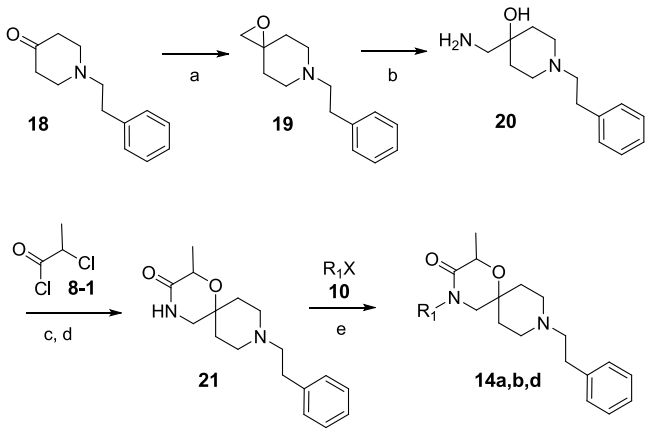

[a]Reagents and conditions: (a) TMSOI, NaH, DMSO, rt to 50 °C, 1 h; (b) NH_3, MeOH, rt, 16 h; (c) K_2CO_3, EtOAc−water, 0 °C, 30 min; (d) ^{t}BuOK, THF, rt, 16 h; (e) NaH, DMF, rt, 16 h.

and heptane) allowed for optical purity enrichment rendering compounds **11R** with ee >98%. Final Boc-deprotection followed by N-alkylation with **13** provided compounds **14** as the *R*-enantiomer with ee >97% (as determined by chiral HPLC).

Following the same sequence described for compound **14u** but starting from the acylating reagent of opposed configuration **8-1R**, the *S*-enantiomer **14x** (Table 4) was obtained.

A single-crystal X-ray diffraction (SCXRD) study of **14u** confirmed the *R* stereochemistry at position 2 (carbon atom labeled as C1 in Figure 2). Since no suitable crystals were obtained using the free base, a limited salt screening was carried out. The hydrobromide provided crystals suitable for SCXRD analysis, from which the absolute configuration was reliably determined by anomalous dispersion effects (Flack parameter = −0.019(8)).

As shown in Figure 3, compound **14u** overlaps well with the MOR and σ_1R pharmacophores used in the generation of the series in the previous work.[2] The ethyl group in position 4 overlaps well with the hydrophobic feature (HYD34) of the σ_1R pharmacophore that was aligned with the aromatic ring feature (AR) of the MOR pharmacophore.

RESULTS AND DISCUSSION

The compounds synthesized were evaluated in a primary σ_1R binding assay using [^{3}H]-(+)-pentazocine[21] as radioligand and in a MOR binding assay using [^{3}H]-DAMGO[2] as radioligand. The MOR functional assay was carried out by measuring cyclic AMP (cAMP) on CHO-K1 cells[22] providing EC_{50} as well as E_{max} data (Tables 1−4). Generally speaking, a full agonist profile is suggested for compounds active at the MOR with E_{max} above 80%. However, a cell line overexpressing the MOR with a high receptor reserve[22] is used in this assay, and thus no unequivocal determination of the functional nature (i.e., full versus partial agonism) can be established and more complex assays are needed such as partial receptor inactivation with *β*-funaltrexamine.[22] The active compounds were also evaluated at 10 *μ*M for hERG blockade and at 1 *μ*M in a selectivity panel constituted by the guinea pig σ_2 receptor (σ2R) and the following human receptors: 5-HT_{1A} receptor, 5-HT_{2B} receptor, α_1A and α_2A adrenoreceptors, dopamine transporter, *δ*-opioid receptor, *κ*-opioid receptor, histamine H_1 receptor, norepinephrine transporter, and serotonin transporter. This panel includes targets validated for pain and others associated with undesirable side effects in order to rule out off-target activities that could interfere with the analgesic response of the compounds. As in the 4-aryl series, selectivity was good and only some of the initial compounds were active for the α_1AR, one of the issues to be improved in this lead optimization program together with hERG inhibition.

The initial work over the 1-oxa-4,9-diazaspiro[5.5]undecan-3-one scaffold indicated that the structural features required to maintain dual activity were the arylethyl group in position 9 (other chain lengths impaired MOR affinity) and the carbonyl oxygen atom in position 3, while substituting position 2 with an alkyl group improved considerably MOR affinity.[2] An aromatic ring in position 4 (R_1) was also initially maintained, according to the superposition of the initial proposal with the MOR pharmacophore, where this ring occupied a nearby position to the phenol ring of morphine. When the current lead optimization program was initiated, we decided to explore the elongation of the distance between the aromatic ring and N_4. Interestingly (Table 1), both targets accommodated a benzyl group (**14a**), although hERG inhibition was worse in relation to **3**. Further elongation to phenethyl (**14b**) was also tolerated by both MOR and σ_1R, although hERG inhibition did not improve. Many different heterocycles were introduced in both benzyl and phenethyl-type derivatives, but either one of the affinities was lost or hERG inhibition did not improve (results not shown).

We decided then to explore the elimination of the aromatic ring in R_1. The cyclopropyl derivative **14c** maintained affinities and provided an improved hERG result, while the simpler alkyl groups isopropyl (**14d**) and ethyl (**14e**) additionally provided a clear reduction in α1AR affinity, which for the first time was below 50% inhibition at 1 *μ*M. The smallest alkyl derivative

Scheme 3[a]

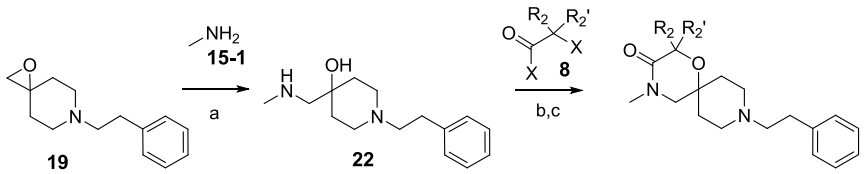

[a]Reagents and conditions: (a) EtOH−water 6:1, rt, 4 h; (b) K_2CO_3, EtOAc−water, 0 °C, 30 min (**14g**), or TEA, DCM, 0 °C, 2 h (**14l**), or $NaHCO_3$, DCM, rt, 16 h (**14m**); (c) ^{t}BuOK, THF, −78 °C to −30 °C, 1−4 h (up to 0 °C, 3 h for **14m**).

https://dx.doi.org/10.1021/acs.jmedchem.0c01127
J. Med. Chem. XXXX, XXX, XXX−XXX

Scheme 4[a]

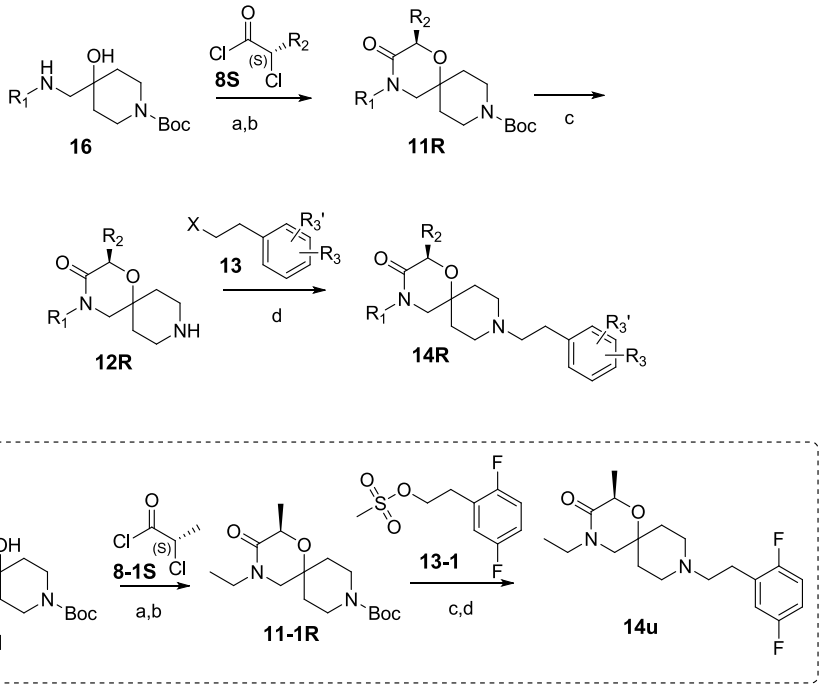

[a]Reagents and conditions: (a) K_2CO_3, EtOAc−water, 0 °C, 30 min; (b) (i) ^{t}BuOK, THF, T < −60 °C, 1 h, (ii) crystallization from AcO^{i}Pr−heptane; (c) TFA, DCM, rt, 3 h; (d) **13**, K_2CO_3, acetonitrile, 80 °C, 16 h.

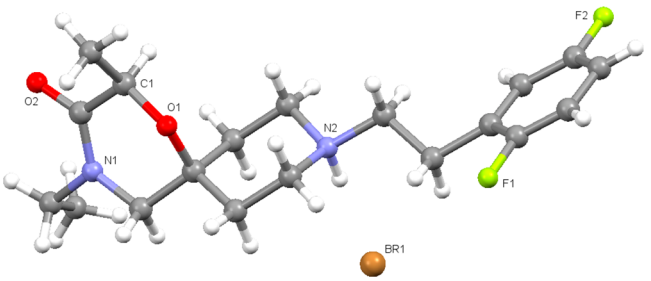

Figure 2. View of the asymmetric unit of the crystal structure of the hydrobromide salt of **14u** (CCDC 1979266), showing the *R* configuration at position 2 (C1 atom).

14f showed a reduced affinity for the primary targets but confirmed the trend toward α_1AR affinity reduction and also provided a hERG IC_{50} above 10 μM, our desired cutoff criteria. This improvement in hERG affinity may well be due to the relevant reduction in lipophilicity of **14f** in relation to **14a**. Finally, the unsubstituted derivative **17** was devoid of any affinity in accordance with the lack of any group covering the HYD34 or AR features of the σ_1R or the MOR pharmacophores, respectively. These results indicated that an alkyl group was tolerated in position 4 and offered a chance for obtaining a dual compound with selectivity for α_1A and hERG.

Maintaining a methyl group in position 4, position 2 (R_2) was modified (Table 2). As in the 4-aryl series, the (*R*)-methyl **14g** was the eutomer regarding MOR affinity, while both enantiomers (**14g** and **14h**) were equipotent for the σ_1R. It was confirmed that the alkyl group in R_2 was indeed necessary for MOR affinity, in view of the low affinity of the unsubstituted analogue **14i**. The alkyl group in R_2 was elongated to ethyl (**14j**) or isopropyl (**14k**), and while the dual affinity was similar to the methyl **14g**, hERG inhibition was higher. In agreement with the results obtained with the 4-aryl derivatives, further elongation of R_2 or introduction of polar groups, such as hydroxyl and carboxylic acid derivatives, was detrimental (results not shown). Direct attachment of a phenyl group in R_2 (**14l**), a substitution that had not been previously explored, also impaired MOR activity. The dimethylated compound **14m** was also poorly active at the MOR receptor, while the spirocyclopropyl **14n** was similar to **14g**. In conclusion, (*R*)-methyl, isopropyl, and spirocyclopropyl were the best possible alternatives in position 2, although the methyl group was more appealing in view of its reduced hERG inhibition.

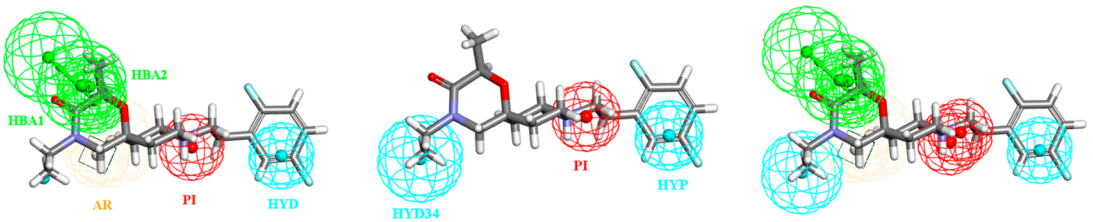

Figure 3. Compound **14u** superimposed onto the MOR (left), σ_1R (middle), and the merged MOR-σ_1R (right) pharmacophores (the AR feature is shown unhighlighted). Pharmacophores were constructed as described in previous work.[2]

https://dx.doi.org/10.1021/acs.jmedchem.0c01127
J. Med. Chem. XXXX, XXX, XXX−XXX

Table 2. Exploration of Substituents in $R_2/R_{2'}$

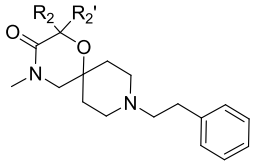

comp	R_2, $R_{2'}$	K_i MOR[a] (*h*, nM)	EC_{50} MOR[b] (*h*, nM)	E_{max} MOR[c] (%)	K_i σ_1R[d] (*h*, nM)	cLogP	hERG[e] IC_{50} (μM)	α_1AR[f] % inh (1 μM)	M[g]
14g	Me, H (*R*)	91 ± 10	319 ± 104	83	277 ± 76	2.2	>10[h]	19	3
14h	Me, H (*S*)	>1000[i]	1780 ± 196		165 ± 55	2.2	NT[j]	6	1[k]
14i	H, H	>1000[i]	>1000[i]		282 ± 48	1.9	NT[j]	36	1
14j	Et, H (*R*)	192 ± 41	505 ± 122	90	139 ± 16	4.1	6.6	13	4
14k	^{i}Pr, H	115 ± 39	174 ± 42	85	122 ± 24	3.1	6.2	29	1
14l	Ph, H	>1000[i]	>1000[i]		242 ± 13	3.4	NT[j]	26	3
14m	Me, Me	>1000[i]	624 ± 35		50 ± 5	2.9	NT[j]	37	3
14n	spirocyclopropyl	221 ± 51	442 ± 65	85	161 ± 43	2.2	3.6	41	N/A[l]

[a,b,c,d,e,f,g,h]See corresponding footnotes of Table 1. [i]Less than 50% inhibition at 1 μM. [j]Not tested. [k]Enantiopure compound (*S* stereochemistry) was obtained by resolution of the racemate **14f** (prepared following Scheme 1) by chiral prep HPLC. [l]Synthesis described in Experimental Section.

Table 3. Refinement of the Phenethyl Substituents $R_3/R_{3'}$

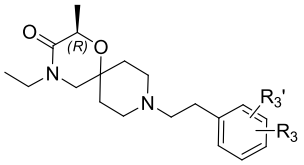

compd	R_3	$R_{3'}$	K_i MOR[a] (*h*, nM)	EC_{50} MOR[b] (*h*, nM)	E_{max} MOR[c] (%)	K_i σ1R[d] (*h*, nM)	cLogP	hERG[e] IC_{50} (μM)	α_1AR[f] % inh (1 μM)	M[g]
14o	H	H	26 ± 4	49 ± 4	83	66 ± 19	2.9	4.7	14	1[h]
14p	2-F	H	18 ± 7	24 ± 3	84	68 ± 18	3.1	4.0	15	4
14q	3-F	H	56 ± 17	56 ± 21	83	64 ± 30	3.1	6.6	42	4
14r	4-F	H	164 ± 29	108 ± 42	81	76 ± 12	3.1	1.5	21	4
14s	2-F	3-F	22 ± 10	10 ± 1	90	556 ± 266	3.1	>10[i]	8	4
14t	2-F	4-F	62 ± 25	53 ± 17	92	94 ± 12	3.2	2.5	11	4
14u	2-F	5-F	64 ± 5	52 ± 1	90	118 ± 7	3.2	>10[i]	21	4
14v	2-F	6-F	21 ± 6	16 ± 1	95	609 ± 253	3.2	NT[j]	10	4

[a,b,c,d,e,f,g]See corresponding footnotes of Table 1. [h]Enantiopure compound was obtained by resolution of the racemate **14e** (prepared following Scheme 1) by chiral prep HPLC. [i]Less than 50% inhibition at 10 μM. [j]Not tested.

Table 4. Miscellaneous Analogues

comp		K_i MOR[a] (*h*, nM)	EC_{50} MOR[b] (*h*, nM)	Emax MOR[c] (%)	K_i σ_1R[d] (*h*, nM)	cLog*P*	hERG[e] IC_{50} (μM)	α_1AR[f] % inh (1 μM)	M[g]
14w	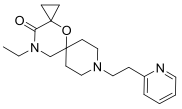	>1000[h]	1498 ± 145	-	783 ± 300	1.2	NT[i]	0	N/A[j]
14x	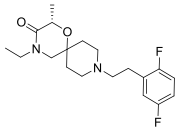	>1000[h]	910 ± 9	-	135 ± 22	3.2	>10[k]	9	4

[a,b,c,d,e,f,g,h]See corresponding footnotes of Table 1. [i]Not tested. [j]Synthesis described in Experimental Section. [k]Less than 50% inhibition at 10 μM.

Regarding the piperidinyl substituent, we knew from the 4-aryl series[2] that the phenethyl length was optimal, since benzyl or alkyl groups led to MOR affinity impairment, and that fluorine was the best substituent to maintain affinity and provide chances of keeping hERG IC_{50} above 10 μM. A wide exploration was undertaken over a matrix of compounds

https://dx.doi.org/10.1021/acs.jmedchem.0c01127
J. Med. Chem. XXXX, XXX, XXX−XXX

composed of the best substituents in position 2 (methyl, ethyl, isopropyl, or spirocyclopropyl) and position 4 (methyl, ethyl, isopropyl, or cyclopropyl). For the sake of the length of the present paper, only detailed SAR over the 4-ethyl-2-methyl derivatives is reported (Table 3). The naked 4-ethyl derivative **14o** improved affinities for the primary targets in relation to its 4-methyl counterpart (**14g**) and maintained selectivity for the α_1AR but showed suboptimal hERG inhibition. The fluoro derivatives **14p−r** maintained dual affinities for MOR and σ_1R but did not improve hERG inhibition. The introduction of a second fluorine atom provided a loss of σ in the 2,3-difluoro (**14s**) and 2,6-difluoro (**14v**) analogues and maintained a good dual profile in the rest. However, only the 2,5-difluoroderivative **14u** showed the desired dual profile with selectivity for the α_1AR and hERG inhibition with IC_{50} above 10 μM. Other substitutions besides fluorine were also assayed, but it was again observed that polar groups were detrimental for the primary affinities, as illustrated by the low MOR affinity of compound **14w** (Table 4), containing a 2-pyridylethyl group, one of the few tolerated polar moieties in our previous work.

Overall, compound **14u** (Figure 4) emerged as the best derivative with the correct functionality for the primary targets.

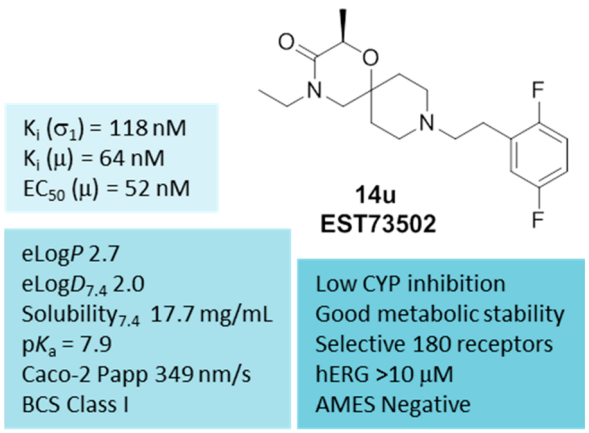

Figure 4. Structure and in vitro profile of the clinical candidate **14u**.

Phenytoin binding experiments[23] showed antagonist behavior for the σ_1R, while β-funaltrexamine experiments[22] showed partial agonist behavior for the MOR (the detailed results will be reported elsewhere soon). Compound **14u** was devoid of hERG inhibition, had low potential for drug−drug interactions based on the low inhibition (<50% at 1 μM) of recombinant human cytochrome P450 (rhCYP) isoforms (1A2, 2C9, 2C19, 2D6, and 3A4),[24] and showed high in vitro metabolic stability in human liver microsomes[25] (Cl_{int} = 2.4 (μL/min)/mg protein). Additionally, compound **14u** did not show in vitro cytotoxic potential in the MTT (3-(4,5-dimethylthiazol-2-yl)-2,5-diphenyltetrazolium bromide) and neutral red uptake assays when tested up to 100 μM in HepG2 cells[26] and lacked genotoxic potential in the SOS/umu and Ames bacterial mutation assays.[27]

Compound **14u** also showed a good physicochemical profile, with moderate basicity (pK_a = 7.9) and lipophilicity (experimental log P = 2.7, log $D_{7.4}$ = 2.0) and very high solubility in the whole physiologically meaningful pH range (thermodynamic solubility of 17.7 mg/mL at pH 7.4 and 45.1 mg/mL at pH 2). This together with its high permeability in Caco-2 cells (349 nm/s) indicates that **14u** will be classified as a BCS class I compound.[28] Compound **14u** complied with Lipinski's rules and was not highly basic, this being a desirable parameter as pointed out by Wager et al.[29] These authors developed the central nervous system multiparameter optimization (CNS MPO) algorithm as a holistic approach for the prediction of good ADME and safety attributes in the case of CNS-directed compounds. An MPO value of 4.4 was calculated for **14u**, which is considered to be in the desirable range. In fact **14u** crosses the BBB, showing an AUC brain/AUC plasma ratio of 2.6 (the complete pharmacokinetic study will be published in due course). This is relevant taking into account that brain exposure is required for opioids to exert antinociceptive effects in acute nociceptive tests[30] and modulation of opioid analgesia by σ_1R is known to occur in brainstem nuclei.[31]

Compound **14u** failed to show any significant affinity (inhibition % at 1 μM of <50%) for another 180 molecular targets (receptors, transporters, ion channels, and enzymes),[32] indicating that it selectively binds to the MOR and σ_1R. Also, in agreement with the general trend of the series, the activity of **14u** for the MOR receptor is quite stereospecific, since its enantiomer (**14x**, Table 4) is almost devoid of affinity.

In order to gain insight into the binding mechanism of compound **14u** in the MOR, its X-ray geometry was docked into the published crystal structure of the active MOR (5C1M).[33] The obtained complex, including the cocrystallized nanobody, was embedded into a POPC bilayer and solvated. After several equilibration steps, a 500 ns molecular dynamic simulation (MD) was run and the resulting trajectory analyzed, showing a good stability, with an average root-mean-square deviation (RMSD) of 2.4 Å and a standard deviation of 0.24 (Figure 5A). The same was done with enantiomer **14x**, and although qualitatively the interactions of both compounds with the receptor are similar, when calculating the average interaction energy throughout the trajectories, **14u** gives a value of −110 kcal/mol whereas a value of −106 kcal/mol was obtained for **14x**. This stronger interaction of **14u** may be a reason for its more favorable binding.

The main polar protein−ligand interactions observed for **14u** are equivalent to those identified for the cocrystallized BU72: A ionic hydrogen bond interaction of the compound's tertiary amine with Asp 147; a highly conserved amino acid in all GPCRs that bind biogenic amines; and a water-mediated interaction of the carbonyl in position 3 with His 297 with a water network that is more extended involving Tyr 148, Lys 233 (characteristic for the MOR active structure). Other observed interactions are depicted in Figure 5B,C.

The antinociceptive activity of compound **14u** was evaluated in the paw pressure test in CD1 male mice (n = 6−12 per group). After oral administration, **14u** showed a dose−response analgesic effect reaching a maximum of 64% and an ED_{50} of 14 mg/kg (Figure 6A). The contribution of the σ_1R to its analgesic effect was evaluated by combined administration with the σ_1R agonist PRE-084 (64 mg/kg, sc). In the presence of PRE-084, **14u** reached a maximal effect of 40%, showing a partial inhibition of its analgesic activity and reaching a plateau effect, in agreement with its partial MOR agonist activity. Conversely, systemic administration of the MOR antagonist naloxone (2 mg/kg, sc) fully reversed the analgesic activity of **14u**, in accordance with previous data demonstrating that blockade of the σ_1R does not inhibit nociceptive pain but potentiates opioid induced analgesia.[9] These data show that both σ_1R and MOR contribute to **14u** analgesic activity.

https://dx.doi.org/10.1021/acs.jmedchem.0c01127
J. Med. Chem. XXXX, XXX, XXX−XXX

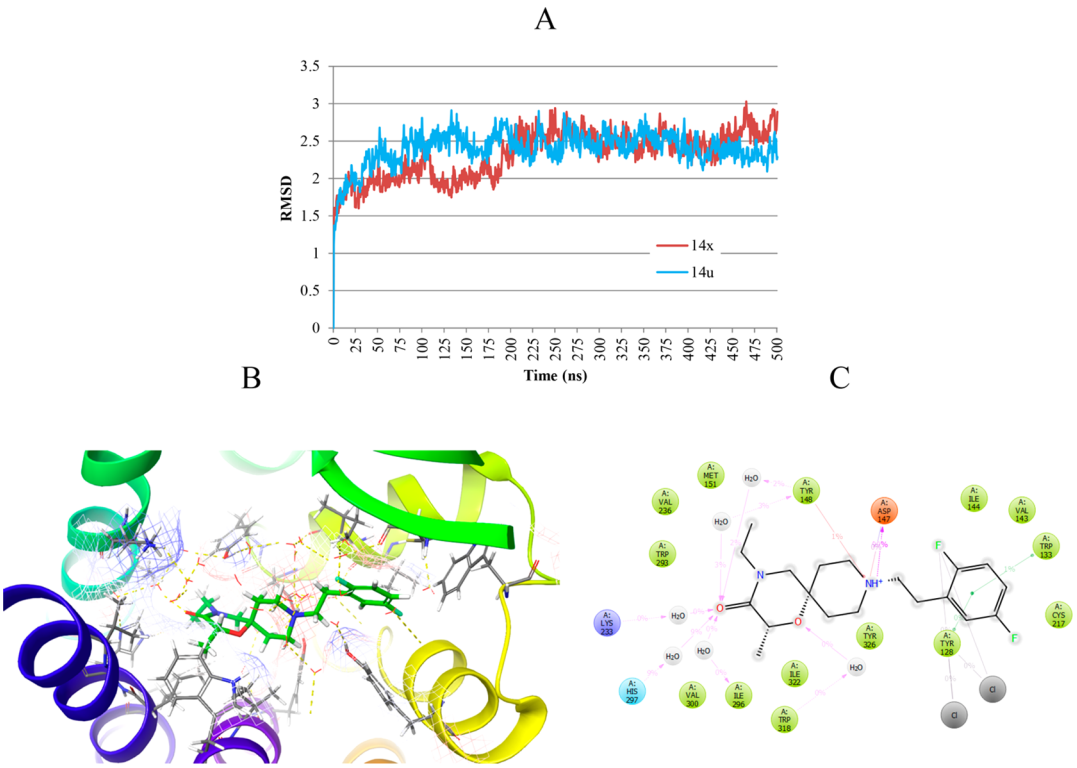

Figure 5. (A) Evolution of the molecular dynamics run for compounds **14u** and **14x** docked in the MOR (5C1M). (B) Docking pose of **14u** in the active MOR (5C1M). (C) 2D diagram of the main interactions of **14u** with the active MOR.

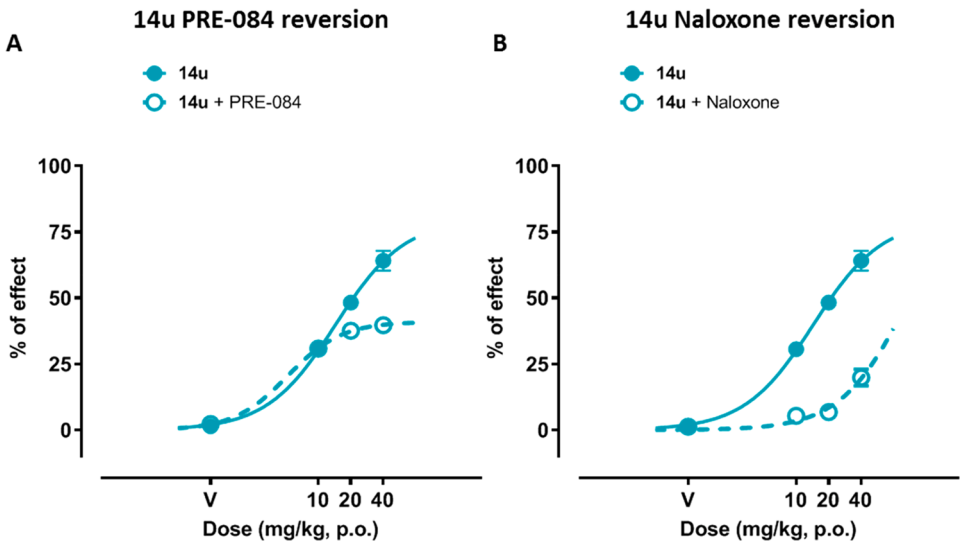

Figure 6. Dose−response antinociception curves in the paw pressure test of **14u** administered alone (filled points) or in the presence of the selective σ_1R agonist PRE084 (empty points, A) and the MOR antagonist naloxone (empty points, B) in male CD1 mice after systemic (po) administration. Each point and vertical line represents the mean ± SEM percentage of effect (n = 6−12 per group).

The analgesic activity of **14u** was also evaluated in the partial sciatic nerve ligation (PSNL) model in CD1 male mice (n = 6−12 per group) in comparison to oxycodone (**1**). The neuropathic pain was evaluated by the mechanical allodynia produced, which was revealed by a decrease in the pressure required to elicit withdrawal of the ipsilateral paw after von Frey filament stimulation on days 5, 13, 18, and 22 after surgery. Compound **14u** (5 mg/kg, ip), oxycodone (**1**, 1.25 mg/kg, ip), or vehicle were repeatedly administered twice a day from day 13 to day 22 after surgery. Both, **14u** and **1** attenuated the expression of mechanical allodynia induced by PSNL, reaching a maximal effect of 56% and 51%, respectively. The effect remained unchanged throughout the treatment duration (Figure 7A).

On day 23 after surgery, the behavioral expression of withdrawal syndrome after repeated treatment was evaluated by naloxone administration (Figure 7B). Using a model previously described and detailed in the experimental part,[34] two classes of behavioral signs were measured: (i) the number of signs and (ii) the presence or absence of each sign during 3 periods of 5 min each. A global score was calculated for each animal as the sum of all behavioral responses. No differences

https://dx.doi.org/10.1021/acs.jmedchem.0c01127
J. Med. Chem. XXXX, XXX, XXX−XXX

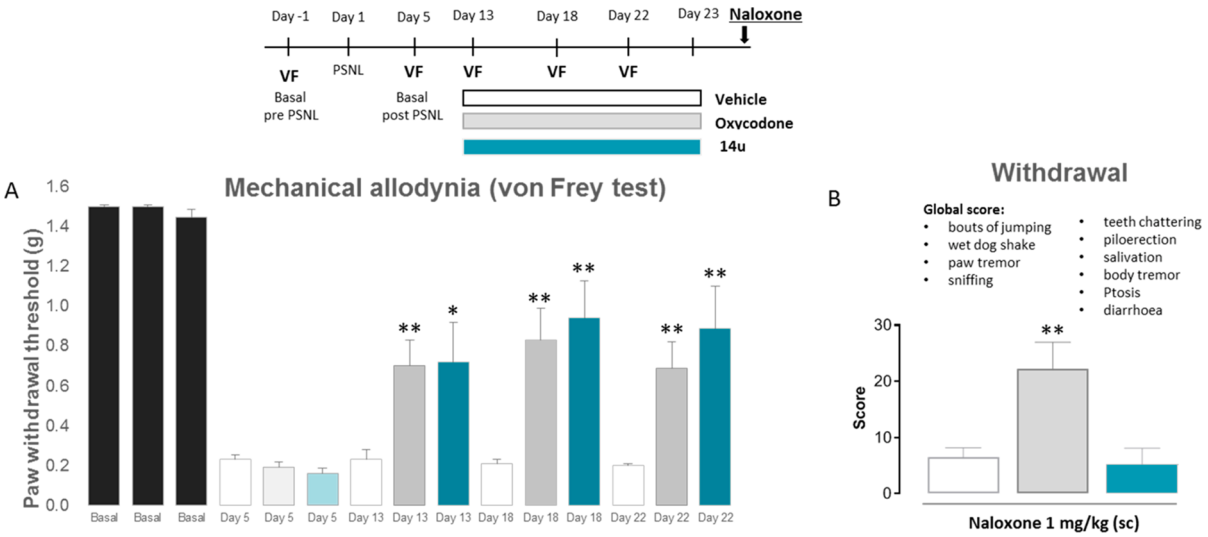

Figure 7. (A) Effect of **14u** (blue bars) or oxycodone (**1**, gray) in comparison to vehicle (white) on PSNL-induced mechanical allodynia in male CD1 mice. Compound **14u** (5 mg/kg) and oxycodone (1.25 mg/kg) were systemically (ip) administered b.i.d. during 10 days. (B) Naloxone precipitated withdrawal response in PSNL mice repeatedly administered with **14u** (blue), oxycodone (gray), or vehicle (white) during 11 days. Naloxone (1 mg/kg, sc) was administered on day 11, 30 min after each treatment administration. The withdrawal response was evaluated immediately after naloxone injection using a global score as described in the Experimental Section. Each bar and vertical line represent the mean ± SEM percentage of effect (n = 6−12 per group): *p < 0.05, **p < 0,01.

between **14u** and vehicle treated groups were observed after naloxone administration. However, oxycodone produced a significant expression of some behavioral signs of opiate withdrawal at the end of treatment, producing an increase in the global withdrawal score. These results demonstrate that, contrary to oxycodone, compound **14u** induced sustained analgesic effect in PSNL mice after repeated administration without expression of naloxone precipitated behavioral signs of opiate withdrawal.

The effect of **14u** on intestinal transit reduction (as a surrogate of constipation) in CD1 mice was also evaluated, as an additional measure of the potential of the compound in showing a reduced opioid-induced side effect profile. The percentage of distance traveled by charcoal meal versus the total length of the small intestine was measured after drug administration in relation to the control group that received vehicle. Systemic administration of compound **14u** elicited a reduced intestinal transit inhibition in mice in comparison with oxycodone at equianalgesic doses (40 mg/kg and 20 mg/kg po, respectively, n = 6−12 per group, Figure 8).

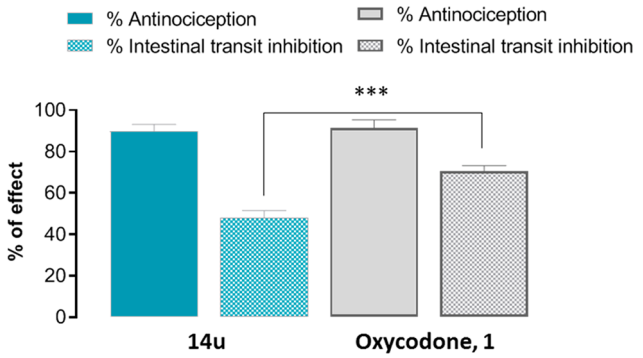

Figure 8. Effect of **14u** (blue bars) or oxycodone (gray bars) on intestinal transit inhibition measured in the charcoal test vs the analgesic response in male CD1 mice after systemic (po) administration. Each bar and vertical line represent the mean ± SEM percentage of effect (n = 6−12 per group): ***p < 0.001.

CONCLUSION

In summary, the synthesis and pharmacological activity of a new series of 4-alkyl-1-oxa-4,9-diazaspiro[5.5]undecane derivatives **14** as potent dual ligands for σ_1R and MOR are reported herein. This family was developed through a lead optimization program over the 4-aryl counterparts, which were designed by using a merging strategy of both target pharmacophores. From the beginning, the series was associated with high hERG inhibition and suboptimal selectivity for the α_1AR. This second item was clearly improved on changing the aryl in position 4 by alkyl groups, but reducing hERG inhibition proved to be much more difficult. In fact, only a handful of derivatives from the hundreds prepared were above the desired threshold (IC_{50} above 10 μM). Among them, compound **14u** selectively binds with the desired functionality to the selected targets, behaving as a partial MOR agonist and σ_1R antagonist. Compound **14u** exhibited analgesic activity in animal models of acute (paw pressure) and chronic (PSNL) pain after single and repeated administration. Both σ_1R and MOR contribute to its antinociceptive effect as it was shown after the combined administration with both the σ_1R agonist PRE-084 and the MOR antagonist naloxone. Contrary to oxycodone, **14u** produces analgesic activity with reduced opioid induced relevant adverse events, like intestinal transit inhibition and naloxone-precipitated behavioral signs of opiate withdrawal.

Compound **14u** (EST73502, (*R*)-9-(2,5-difluorophenethyl)-4-ethyl-2-methyl-1-oxa-4,9-diazaspiro[5.5]undecan-3-one) was selected as a clinical candidate for the treatment of pain in view of its potential to provide good analgesic efficacy with a substantially reduced adverse event profile in relation to the standards of care. Phase 1 clinical trials are underway and will be reported in due course.[35]

https://dx.doi.org/10.1021/acs.jmedchem.0c01127
J. Med. Chem. XXXX, XXX, XXX−XXX

EXPERIMENTAL SECTION

Unless otherwise noted, all materials were obtained from commercial suppliers and used without further purification. Flash chromatography was performed on a Teledyne Isco CombiFlash RF system with disposable columns. ^{1}H spectra were recorded on a Varian Mercury 400 MHz (spectrometer fitted with a 5 mm ATB 1H/19F/X probe) with 2 H lock in deuterated solvents. Chemical shifts (δ) are in parts per million. Commercially available reagents and solvents (HPLC grade) were used without further purification for all the analytical tests. Analytical HPLC−MS for all final compounds and intermediates was performed on an Agilent HP1200-MS 6110 system. A reverse phase XBridge C18 XP column was used (4.6 mm × 30 mm, 2.5 μm), gradient 5−100% B (A = 10 mM ammonium bicarbonate, B = acetonitrile) over 8 min, injection volume 1 μL, flow 2.0 mL/min, temperature 40 °C. UV spectra were recorded at 210 nm using an Agilent HP1200 VWD detector. Mass spectra were obtained over the range m/z 50−1000 by electron spray ionization (ESI) in positive mode using Agilent MS6110 simple quadrupole. Data were integrated and reported using Agilent ChemStation software. All compounds displayed purity higher than 95% as determined by this method, with the exception of compound **14n**, whose purity was 94%. Accurate mass measurements were carried out using an Agilent 6540 UHD Accurate-Mass QTOF system and obtained by electron spray ionization (ESI) in positive mode. Chiral analytical and preparative HPLC was performed in Agilent 1100 analytical and preparative HPLC systems, respectively. The coated or immobilized polysaccharide columns were acquired from Chiral Technologies Europe; heptane and ethanol or IPA with or without DEA at variable proportions were used as mobile phases. All compounds active in biological assays were electronically filtered for structural attributes common to pan assay interference compounds (PAINS) and were found to be negative.[36]

Determination of Physicochemical Properties. p*K*a was calculated using ACDLABS 9.0.3 and cLogP using ChemDraw Ultra 10.0.3. Solubility was measured as thermodynamic solubility from solid compound in phosphate buffer at pH = 7.4 by HPLC. The log *P* and p*K*a were determined by using a pHmetric technique[37] in a GlpKa or a Sirius-T3 Analytical instrument.

(*S*)-2-Chloropropanoyl Chloride (8-1S). To a solution of (*S*)-2-chloropropanoic acid (100.00 g, 0.92 mol) in DCM (1.2 L) under a nitrogen atmosphere, DMF (2 mL) was added. Then, a solution of oxalyl chloride (83 mL, 0.97 mol) in DCM (250 mL) was added dropwise over 30 min, maintaining the internal temperature below 25 °C. After stirring for additional 2.5 h at rt, the solvent was evaporated under vacuum (bath temperature below 15 °C as the product is volatile) to give (*S*)-2-chloropropanoyl chloride (**8-1S**) as a pale yellow oil (115.90 g, 99% yield). ^{1}H NMR (400 MHz, $CDCl_3$,) δ 4.66 (q, J = 7.0 Hz, 1H), 1.82 (d, J = 6.8 Hz, 3H).

2,5-Difluorophenethyl Methanesulfonate (13-1). A solution of 2-(2,5-difluorophenyl)ethanol (22.42 g, 0.14 mol) in DCM (224 mL) was cooled to −10 °C under a nitrogen atmosphere. TEA (20 mL, 0.14 mol) was added dropwise, maintaining the internal temperature below −5 °C. Then, methanesulfonyl chloride (11.1 mL, 0.14 mol) was added dropwise, maintaining the internal temperature below −5 °C. When the addition was completed, a white precipitate appeared. The resulting mixture was stirred for additional 2 h at rt. IPC (TLC, DCM/MeOH 9/1) was performed to monitor full conversion. Saturated aqueous $NaHCO_3$ was then added, and the resulting mixture was stirred for 1 h at rt. Then, it was extracted three times with DCM. The combined organic phases were washed with brine, dried over Na_2SO_4, filtered, and concentrated to dryness to give 2,5-difluorophenethyl methanesulfonate (**13-1**) as a yellow oil (28.03 g, 91% yield). ^{1}H NMR (400 MHz, $CDCl_3$) δ 7.10−6.90 (m, 3H), 4.43 (t, J = 6.7 Hz, 2H), 3.08 (t, J = 6.7 Hz, 2H), 2.94 (s, 3H).

General Procedures for the Synthesis of 4-Alkyl-1-oxa-4,9-diazaspiro[5.5]undecane Derivatives 14. 4-Isopropyl-2-methyl-9-phenethyl-1-oxa-4,9-diazaspiro[5.5]undecan-3-one (14d) (Representative Example of Scheme 2). Step 1: To a suspension of trimethylsulfoxonium iodide (13.00 g, 59.07 mmol) and NaH (2.36 g, 60 wt % in mineral oil, 59.00 mmol) in dry DMSO (70 mL), a solution of 1-phenethylpiperidin-4-one (**18**, 10.00 g, 49.19 mmol) in dry DMSO (70 mL) was added dropwise. The reaction mixture was stirred at rt for 30 min, then it was heated at 50 °C for 1 h. After cooling to rt, ice was slowly added, and the reaction mixture was extracted three times with ethyl acetate. The organic phases were combined, washed with water, dried over $MgSO_4$, filtered, and concentrated under vacuum to give 6-phenethyl-1-oxa-6-azaspiro[2.5]octane (**19**) as an orange oil (8.24 g, 77%). ^{1}H NMR (400 MHz, $CDCl_3$) δ 7.31−7.25 (m, 2H), 7.23−7.17 (m, 3H), 2.87−2.79 (m, 2H), 2.74−2.58 (m, 8H), 1.88 (ddd, J = 13.2, 9.0, 4.3 Hz, 2H), 1.63−1.53 (m, 2H). HPLC−MS: purity 99%, m/z = 218.1 $[M + H]^+$.

Step 2: A mixture of **19** (4.00 g, 18.41 mmol) and ammonia solution (79 mL, 7 M solution in MeOH, 0.55 mol) was stirred at rt overnight. The solvent was removed under vacuum to give 4-(aminomethyl)-1-phenethylpiperidin-4-ol (**20**) as a yellow oil (4.31 g, quantitative). ^{1}H NMR (400 MHz, $CDCl_3$) δ 7.30−7.25 (m, 2H), 7.22−7.15 (m, 3H), 2.85−2.79 (m, 2H), 2.76 (dt, J = 7.0, 3.2 Hz, 2H), 2.66−2.59 (m, 4H), 2.44 (td, J = 10.8, 4.7 Hz, 2H), 1.66−1.54 (m, 4H). HPLC−MS: purity 90%, m/z = 235.1 $[M + H]^+$.

Step 3: To a solution of **20** (4.95 g, 21.12 mmol) in ethyl acetate (45 mL), a solution of K_2CO_3 (7.33 g, 53.03 mmol) in water (35 mL) was added. After cooling to 0 °C, 2-chloropropionyl chloride (**8-1**, 2.5 mL, 25.75 mmol) was added dropwise and the reaction mixture was stirred at 0 °C for 30 min. The layers were separated, and the aqueous phase was extracted with ethyl acetate. The combined organic phases were dried over $MgSO_4$, filtered, and concentrated to dryness to give crude 2-chloro-*N*-((4-hydroxy-1-phenethylpiperidin-4-yl)methyl)-propanamide as an orange oil (6.00 g, 88%), which was used without further purification. To a solution of potassium *tert*-butoxide (31.3 mL, 1 M in THF, 31.30 mmol) in THF (35 mL), a solution of crude 2-chloro-*N*-((4-hydroxy-1-phenethylpiperidin-4-yl)methyl)-propanamide (6.00 g, 18.47 mmol) in THF (100 mL) was added dropwise over 3 h. The reaction mixture was stirred at rt overnight. The solvent was removed under vacuum, water was added to the residue, and it was extracted with ethyl acetate. The combined organic phases were dried over $MgSO_4$, filtered, and concentrated to dryness. The residue was purified by flash chromatography (SiO_2, DCM/MeOH up to 20%) to give 2-methyl-9-phenethyl-1-oxa-4,9-diazaspiro[5.5]undecan-3-one (**21**) as a beige solid (2.30 g, 42%). ^{1}H NMR (400 MHz, $CDCl_3$) δ 7.32−7.26 (m, 2H), 7.23−7.17 (m, 3H), 6.10 (br s, 1H, NH), 4.21 (q, J = 6.8 Hz, 1H), 3.37 (d, J = 11.9 Hz, 1H), 3.12 (dd, J = 11.9, 4.8 Hz, 1H), 2.85−2.78 (m, 2H), 2.74−2.67 (m, 1H), 2.67−2.60 (m, 2H), 2.59−2.48 (m, 1H), 2.35 (td, J = 11.2, 2.1 Hz, 1H), 2.20 (d, J = 14.0 Hz, 1H), 1.77−1.61 (m, 4H), 1.46 (d, J = 6.8 Hz, 3H). HPLC−MS: purity 100%, m/z = 289.1 $[M + H]^+$.

Step 4: To a solution of **21** (168 mg, 0.58 mmol) in dry DMF (5 mL), NaH (47 mg, 60 wt % in mineral oil, 1.17 mmol) was added. The reaction mixture was stirred at rt for 30 min, then 2-bromopropane (0.05 mL, 0.58 mmol) was added and the resulting mixture was stirred at rt overnight. Water was added, and it was extracted with ethyl acetate. The organic phases were combined, washed with brine, dried over $MgSO_4$, filtered, and concentrated to dryness. The residue was purified by flash chromatography (SiO_2, DCM/MeOH up to 20%) to obtain 4-isopropyl-2-methyl-9-phenethyl-1-oxa-4,9-diazaspiro[5.5]undecan-3-one (**14d**) as a colorless oil (84 mg, 43%). ^{1}H NMR (400 MHz, $CDCl_3$) δ 7.32−7.26 (m, 2H), 7.23−7.17 (m, 3H), 4.86 (sept, J = 6.8 Hz, 1H), 4.17 (q, J = 6.8 Hz, 1H), 3.15 (d, J = 12.3 Hz, 1H), 2.96 (d, J = 12.3 Hz, 1H), 2.87−2.79 (m, 2H), 2.75−2.60 (m, 4H), 2.60−2.43 (m, 1H), 2.36 (t, J = 10.1 Hz, 1H), 2.03 (d, J = 14.5 Hz, 1H), 1.75−1.67 (m, 2H), 1.63−1.49 (m, 1H), 1.44 (d, J = 6.8 Hz, 3H), 1.11 (d, J = 6.9 Hz, 3H), 1.07 (d, J = 6.7 Hz, 3H). HPLC−MS: purity 99%. HRMS $[M + H]^+$ (diff ppm) 331.2379 (0.34).

2,4-Dimethyl-9-phenethyl-1-oxa-4,9-diazaspiro[5.5]-undecan-3-one Hydrochloride (14f) (Representative Example of Scheme 1 Using Variation from Compound 7). Step 1:[18] To a suspension of potassium *tert*-butoxide (73.20 g, 0.65 mol) in DMSO

https://dx.doi.org/10.1021/acs.jmedchem.0c01127
J. Med. Chem. XXXX, XXX, XXX−XXX

(550 mL), trimethylsulfoxonium iodide (160.16 g, 0.73 mol) was added portionwise in 20 min, maintaining the internal temperature between 20 and 25 °C. The reaction mixture (pale yellow solution) was stirred at rt for 90 min, then DME (150 mL) was added, and it was cooled to 0−5 °C. A solution of *tert*-butyl 4-oxopiperidine-1-carboxylate (**5**, 100.00 g, 0.50 mol) in a mixture of DMSO/DME (1/3, 200 mL) was added dropwise over 35 min, maintaining the reaction temperature below 5 °C. The reaction mixture (yellow solution) was stirred at 0−5 °C for additional 60 min. IPC (TLC, cyclohexane/ethyl acetate 7/3) was performed to monitor full conversion. Ethyl acetate (400 mL) and water (600 mL) were then added, and the reaction mixture was stirred for 20 min. The phases were separated, and the aqueous layer was extracted with ethyl acetate (2 × 400 mL). The organic phases were combined, washed with water (4 × 400 mL), dried over $MgSO_4$, filtered, and concentrated under vacuum to give *tert*-butyl 1-oxa-6-azaspiro[2.5]octane-6-carboxylate (**6**) as a white solid (97.60 g, 91% yield). ^{1}H NMR (400 MHz, $CDCl_3$) δ 3.77−3.63 (m, 2H), 3.42 (ddd, J = 13.3, 9.5, 3.7 Hz, 2H), 2.68 (s, 2H), 1.79 (ddd, J = 13.7, 9.5, 4.4 Hz, 2H), 1.46 (s, 9H), 1.44−1.40 (m, 2H). HPLC−MS: purity 98%, m/z = 158.1 $[M + H - 56]^+$ (-^{t}Bu, Boc fragmentation).

Step 2: A mixture of **6** (16.67 g, 78.16 mmol) and ammonia solution (39 mL, 7 M solution in MeOH, 2.34 mol) was stirred at rt overnight. The solvent was removed under vacuum and the residue was purified by flash chromatography (SiO_2, DCM/MeOH up to 20%) to give *tert*-butyl 4-(aminomethyl)-4-hydroxypiperidine-1-carboxylate (**7**) as a yellow oil (13.39 g, 74%). ^{1}H NMR (400 MHz, $CDCl_3$) 3.86 (br s, 2H), 3.17 (t, J = 12.0 Hz, 2H), 2.60 (s, 2H), 1.51 (d, J = 12.4 Hz, 2H), 1.46 (s, 9H), 1.43−1.32 (m, 2H). HPLC−MS: purity 97%, m/z = 175.1 $[M + H - 56]^+$ (-^{t}Bu, Boc fragmentation).

Step 3: To a solution of **7** (9.50 g, 41.25 mmol) in ethyl acetate (85 mL), a solution of K_2CO_3 (15.90 g, 115.04 mmol) in water (66 mL) was added. After cooling to 0 °C, 2-chloropropionyl chloride (**8-1**, 5.4 mL, 56.09 mmol) was added dropwise and the reaction mixture was stirred at 0 °C for further 30 min. The layers were separated, and the aqueous phase was extracted with ethyl acetate. The combined organic phases were dried over $MgSO_4$, filtered, and concentrated to dryness to give crude *tert*-butyl 4-((2-chloropropanamido)methyl)-4-hydroxypiperidine-1-carboxylate as a yellow oil (12.20 g, 92%), which was used without purification. To a solution of potassium *tert*-butoxide (62.7 mL, 1 M in THF, 62.70 mmol) in a mixture of THF (164 mL) and *tert*-butanol (82 mL), warmed at 80 °C, a solution of the previous crude *tert*-butyl 4-((2-chloropropanamido)methyl)-4-hydroxypiperidine-1-carboxylate (12.20 g, 38.03 mmol) in THF (205 mL) was added dropwise over 3 h. The reaction mixture was stirred at rt overnight. The solvent was removed under vacuum, water was added to the residue, and it was extracted with ethyl acetate. The combined organic phases were dried over $MgSO_4$, filtered, and concentrated to dryness to give *tert*-butyl 2-methyl-3-oxo-1-oxa-4,9-diazaspiro[5.5]undecane-9-carboxylate (**9-1**) as a white solid (9.29 g, 86%). ^{1}H NMR (400 MHz, $CDCl_3$) δ 5.75 (br s, 1H, NH), 4.20 (q, J = 6.8 Hz, 1H), 3.82 (br s, 2H), 3.38 (d, J = 12.0 Hz, 1H), 3.26 (t, J = 11.9 Hz, 1H), 3.10 (dd, J = 11.9, 4.8 Hz, 1H), 3.05 (t, J = 11.0 Hz, 1H), 2.16 (d, J = 15.2 Hz, 1H), 1.67−1.49 (m, 3H), 1.46 (s, 9H), 1.46 (d, J = 6.8 Hz, 3H). HPLC−MS: purity 94%, m/z = 229.1 $[M + H - 56]^+$ (-^{t}Bu, Boc fragmentation).

Step 4: To a solution of **9-1** (1.00 g, 3.52 mmol) in dry DMF (25 mL), NaH (0.28 g, 60 wt % in mineral oil, 7.03 mmol) was added under a nitrogen atmosphere. The mixture was stirred at rt for 30 min, then iodomethane (0.22 mL, 3.52 mmol) was added and the resulting mixture was stirred at rt overnight. Water was added, and it was extracted with ethyl acetate. The organic phases were combined, washed with brine, dried over $MgSO_4$, filtered, and concentrated to dryness to obtain *tert*-butyl 2,4-dimethyl-3-oxo-1-oxa-4,9-diazaspiro[5.5]undecane-9-carboxylate (**11-2**) as a yellow oil (765 mg, 73%). ^{1}H NMR (400 MHz, $CDCl_3$) δ 4.17 (q, J = 6.7 Hz, 1H), 3.82 (br s, 2H), 3.42 (d, J = 12.2 Hz, 1H), 3.24 (t, J = 11.2 Hz, 1H), 3.03 (t, J = 11.4 Hz, 1H), 2.97 (d, J = 12.1 Hz, 1H), 2.97 (s, 3H), 2.15−2.06 (m, 1H), 1.63−1.50 (m, 2H), 1.46 (s, 9H), 1.44 (d, J = 6.8 Hz, 3H), 1.44−1.39 (m, 1H). HPLC−MS: purity 91%, m/z = 299.1 $[M + H]^+$.

Step 5: To a solution of **11-2** (765 mg, 2.56 mmol) in DCM (8 mL), trifluoroacetic acid (0.99 mL, 12.80 mmol) was added, and the reaction mixture was stirred at rt overnight. Then it was evaporated to dryness to give crude 2,4-dimethyl-1-oxa-4,9-diazaspiro[5.5]undecan-3-one trifluoroacetate (**12-2** TFA salt) as a viscous oil (1.26 g, overweight, estimated 64 wt %; theoretical weight 0.80 g; quantitative yield was assumed) that was used in the following step without further purification. ^{1}H NMR (400 MHz, $CDCl_3$) δ 8.59 (br s, 2H), 4.22 (q, J = 6.7 Hz, 1H), 3.53 (d, J = 12.7 Hz, 1H), 3.45−3.31 (m, 3H), 3.20−3.08 (m, 1H), 3.13 (d, J = 12.7 Hz, 1H), 3.03 (s, 3H), 2.36 (d, J = 15.2 Hz, 1H), 2.08−1.96 (m, 1H), 1.93−1.82 (m, 2H), 1.47 (d, J = 6.8 Hz, 3H). HPLC−MS: purity 100%, m/z= 199.1 $[M + H]^+$.

Step 6: A mixture of **12-2** TFA salt (1.26 g, 64 wt %, 2.56 mmol), (2-bromoethyl)benzene (0.35 mL, 2.58 mmol), sodium iodide (0.23 g, 1.55 mmol), and *N*,*N*-diisopropylethylamine (2.25 mL, 12.9 mmol) in acetonitrile (32 mL) was heated at 80 °C in a sealed tube overnight. Water was added, and it was extracted with ethyl acetate. The combined organic phases were washed with brine, dried over $MgSO_4$, filtered, and concentrated to dryness. The residue was purified by flash chromatography (SiO_2, DCM/MeOH up to 10%) to obtain 2,4-dimethyl-9-phenethyl-1-oxa-4,9-diazaspiro[5.5]undecan-3-one (**14f** free base) as an oil (486 mg, 62%). To a solution of the previous free base (50 mg, 0.16 mmol) in anhydrous diethyl ether (0.5 mL), HCl (2 M solution in diethyl ether, 0.09 mL, 0.18 mmol) was added, and the mixture was stirred at rt for 2 h. The solids were filtered and dried in vacuo to give **14f** HCl salt as a white solid (32 mg, 57%). ^{1}H NMR (400 MHz, CD_3OD) δ 7.40−7.24 (m, 5H), 4.24 (q, J = 6.7 Hz, 1H), 3.62−3.51 (m, 3H), 3.44−3.34 (m, 3H), 3.28−3.15 (m, 2H), 3.14−3.05 (m, 2H), 2.99 (s, 3H), 2.45 (d, J = 14.1 Hz, 1H), 2.02 (t, J = 13.9 Hz, 1H), 1.96−1.80 (m, 2H), 1.42 (d, J = 6.7 Hz, 3H). HPLC−MS: purity 97%. HRMS $[M + H]^+$ (diff ppm) 303.2072 (−1.6).

(*R*)-2,4-Dimethyl-9-phenethyl-1-oxa-4,9-diazaspiro[5.5]-undecan-3-one Hydrochloride (14g) (Representative Example of Scheme 3, Chiral Version). Step 1: To a solution of 6-phenethyl-1-oxa-6-azaspiro[2.5]octane (**19**, 3.78 g, 17.39 mmol) in a mixture of EtOH (90 mL) and water (16 mL), methylamine solution (30 mL, 40 wt % in water, 0.35 mol) was added, and the reaction mixture was stirred at rt for 4 h. The solvent was removed under vacuum to give 4-((methylamino)methyl)-1-phenethylpiperidin-4-ol (**22**) as a pale orange solid (4.35 g, quantitative). ^{1}H NMR (400 MHz, $CDCl_3$) δ 7.31−7.26 (m, 2H), 7.23−7.17 (m, 3H), 2.88−2.76 (m, 4H), 2.69−2.60 (m, 2H), 2.53 (s, 2H), 2.49 (s, 3H), 2.53−2.44 (m, 2H), 1.70−1.57 (m, 4H). HPLC−MS: purity 100%, m/z = 249.1 $[M + H]^+$.

Step 2: To a solution of **22** (500 mg, 2.01 mmol) in ethyl acetate (8 mL), a solution of K_2CO_3 (779 mg, 5.64 mmol) in water (7 mL) was added. After cooling to 0 °C, a solution of (*S*)-2-chloropropanoyl chloride (**8-1S**, 307 mg, 2.41 mmol) in EtOAc (3 mL) was added dropwise, and the reaction mixture was stirred at 0 °C for 30 min. Then, the layers were separated and the aqueous phase was extracted with ethyl acetate. The organic phases were combined, washed with saturated aqueous $NaHCO_3$, dried over $MgSO_4$, filtered, and concentrated to dryness to give crude (*S*)-2-chloro-*N*-((4-hydroxy-1-phenethylpiperidin-4-yl)methyl)-*N*-methylpropanamide (500 mg, 73%). A solution of the previous crude compound (500 mg, 1.47 mmol) in THF (15 mL) was cooled to −78 °C using a dry ice/acetone bath. Then, a solution of potassium *tert*-butoxide (1.62 mL, 1 M in THF, 1.62 mmol) was added dropwise, and the reaction mixture was stirred at −78 °C for 30 min. NH_4Cl saturated solution was then added, and the reaction mixture was warmed to rt and extracted with ethyl acetate. The organic phases were combined, dried over $MgSO_4$, filtered, and concentrated under vacuum to give crude (*R*)-2,4-dimethyl-9-phenethyl-1-oxa-4,9-diazaspiro[5.5]undecan-3-one (**14g** free base) as an oil (400 mg, 90%) with ee 93% (chiral HPLC).

Step 3: To a solution of **14g** free base (1.56 g, 5.16 mmol, ee 92.4%) in diethyl ether (4 mL), a solution of HCl (2.58 mL, 2 M in diethyl ether, 5.16 mmol) was added under stirring, upon which a solid started to precipitate immediately. The resulting suspension was

https://dx.doi.org/10.1021/acs.jmedchem.0c01127
J. Med. Chem. XXXX, XXX, XXX−XXX

stirred for 1 h at rt, and then it was concentrated to dryness to obtain crude **14g** HCl salt as a white solid (1.49 g, 86% yield). The crude product was crystallized from hot acetonitrile/ethyl acetate mixture to enrich ee %: acetonitrile (30 mL) was added to crude **14g** HCl salt (1.49 g), and the mixture was heated to reflux until total solution. Ethyl acetate (119 mL) was added while hot, and the solution was allowed to cool down to rt (crystallization started at 35−38 °C) and further stirred at rt for 2.5 h. Then, the solids were collected by filtration and dried under vacuo to give **14g** HCl salt as a white solid (717 mg, 48%) with ee 98.1% (chiral HPLC). ^{1}H NMR (400 MHz, CD_3OD) δ 7.42−7.24 (m, 5H), 4.24 (q, J = 6.7 Hz, 1H), 3.61−3.52 (m, 3H), 3.42−3.33 (m, 3H), 3.27−3.15 (m, 2H), 3.14−3.08 (m, 2H), 2.98 (s, 3H), 2.45 (ddd, J = 15.5, 5.3, 2.7 Hz, 1H), 2.10−1.99 (m, 1H), 1.95−1.84 (m, 2H), 1.42 (d, J = 6.7 Hz, 3H). HPLC−MS: purity 100%. HRMS $[M + H]^+$ (diff ppm) 303.2078 (−3.65).

(*S*)-2,4-Dimethyl-9-phenethyl-1-oxa-4,9-diazaspiro[5.5]-undecan-3-one Hydrochloride (14h). Starting from racemic 2,4-dimethyl-9-phenethyl-1-oxa-4,9-diazaspiro[5.5]undecan-3-one (**14f**, 428 mg), a chiral preparative HPLC separation (column CHIRALCEL OJ; temperature ambient; flow 11 mL/min; eluent *n*-heptane/(IPA + 0.33% DEA) 95/5 v/v) was carried out to give (*S*)-2,4-dimethyl-9-phenethyl-1-oxa-4,9-diazaspiro[5.5]undecan-3-one (**14h**) as a colorless oil (41 mg) with ee 96.1% (chiral HPLC). Its *R*-enantiomer (**14g**) was also recovered as a colorless oil (127 mg) with ee 94.5% (chiral HPLC). Absolute configuration was assigned using a sample of compound **14g** obtained as described above.

To a solution of **14h** free base (41 mg, 0.13 mmol) in anhydrous diethyl ether (1 mL), HCl (2 M solution in diethyl ether, 0.09 mL, 0.18 mmol) was added. The mixture was stirred at rt for 1 h, and then it was concentrated to dryness to give **14h** HCl salt as a white solid (35 mg, 76%). ^{1}H NMR (400 MHz, CD_3OD) δ 7.40−7.25 (m, 5H), 4.25 (q, J = 6.7 Hz, 1H), 3.61−3.49 (m, 3H), 3.44−3.34 (m, 3H), 3.28−3.17 (m, 2H), 3.14−3.06 (m, 2H), 2.99 (s, 3H), 2.44 (br d, J = 14.2 Hz, 1H), 2.06−1.96 (m, 1H), 1.96−1.82 (m, 2H), 1.42 (d, J = 6.7 Hz, 3H). HPLC−MS: purity 100%. HRMS $[M + H]^+$ (diff ppm) 303.2071 (−1.17).

4-Methyl-9-phenethyl-1-oxa-4,9-diazaspiro[5.5]undecan-3-one Hydrochloride (14i) (Representative Example of Scheme 1 Using Variation from Compound 16). Step 1: To a solution of *tert*-butyl 1-oxa-6-azaspiro[2.5]octane-6-carboxylate (**6**, 41.37 g, 0.19 mol) in a mixture of EtOH−water 9:1 (850 mL), methylamine solution (456 mL, 33% solution in EtOH, 3.88 mol) was added. The reaction mixture was stirred at rt overnight. The solvent was removed under vacuum to give *tert*-butyl 4-hydroxy-4-((methylamino)methyl)-piperidine-1-carboxylate (**16-2**) as a pale yellow solid (46.88 g, 99%). ^{1}H NMR (400 MHz, $CDCl_3$) δ 3.82 (br s, 2H), 3.15 (t, J = 11.5 Hz, 2H), 2.49 (s, 2H), 2.47 (s, 3H), 1.44 (s, 9H), 1.54−1.34 (m, 4H). HPLC−MS: purity 99%, m/z = 245.1 $[M + H]^+$.

Step 2: To a solution of **16-2** (300 mg, 1.23 mmol) in ethyl acetate (5.4 mL), a solution of K_2CO_3 (475 mg, 3.44 mmol) in water (4.4 mL) was added. After cooling to 0−5 °C, a solution of 2-chloroacetyl chloride (0.13 mL, 1.67 mmol) in EtOAc (0.5 mL) was added dropwise and the reaction mixture was stirred at 0−5 °C for 30 min. Then, saturated aqueous $NaHCO_3$ was added, the layers were separated, and the aqueous phase was extracted with ethyl acetate. The organic phases were combined, washed with brine, dried over $MgSO_4$, filtered, and concentrated to dryness to give crude *tert*-butyl 4-((2-chloro-*N*-methylacetamido)methyl)-4-hydroxypiperidine-1-carboxylate as a white solid (375 mg, 95%). A solution of the previous crude compound (375 mg, 1.17 mmol) in THF (20 mL) was cooled to −78 °C using a dry ice/acetone bath. Then, a solution of potassium *tert*-butoxide (1.52 mL, 1 M in THF, 1.52 mmol) was added dropwise, and the reaction mixture was stirred at −78 °C for 30 min. NH_4Cl saturated solution was then added, the reaction mixture was warmed to rt, and it was extracted with ethyl acetate. The organic phases were combined, dried over $MgSO_4$, filtered, and concentrated under vacuum to give *tert*-butyl 4-methyl-3-oxo-1-oxa-4,9-diazaspiro[5.5]undecane-9-carboxylate (**11-3**) as an oil that solidified upon standing (343 mg, quantitative). ^{1}H NMR (400 MHz, $CDCl_3$) δ 4.14 (s, 2H), 3.84 (s, 2H), 3.19 (s, 2H), 3.10 (t, J = 12.4 Hz, 2H), 2.99 (s, 3H), 1.88 (d, J = 12.1 Hz, 2H), 1.56−1.47 (m, 2H), 1.46 (s, 9H). HPLC−MS: purity 91%, m/z = 285.1 $[M + H]^+$.

Step 3: To a solution of **11-3** (332 mg, 1.17 mmol) in DCM (16 mL), trifluoroacetic acid (0.90 mL, 11.69 mmol) was added. The reaction mixture was stirred at rt for 3 h, and then it was evaporated to dryness to give crude 4-methyl-1-oxa-4,9-diazaspiro[5.5]undecan-3-one trifluoroacetate (**12-3** TFA salt) as a viscous oil (686 mg, overweight, estimated 50 wt %; theoretical weight 349 mg; quantitative yield was assumed) that was used in the following step without further purification. ^{1}H NMR (400 MHz, $CDCl_3$) δ 8.73 (br s, 1H), 8.61 (br s, 1H), 4.23 (s, 2H), 3.40 (d, J = 12.5 Hz, 2H), 3.32 (s, 2H), 3.23 (dd, J = 22.8, 11.4 Hz, 2H), 3.05 (s, 3H), 2.14 (d, J = 14.3 Hz, 2H), 1.99 (td, J = 14.6, 3.7 Hz, 2H). HPLC−MS: purity 100%, m/z= 185.1 $[M + H]^+$.

Step 4: A mixture of **12-3** TFA salt (686 mg, 50 wt %, 1.17 mmol), (2-bromoethyl)benzene (260 mg, 1.40 mmol) and K_2CO_3 (808 mg, 5.85 mmol) in acetonitrile (10 mL) were heated at 80 °C in a sealed tube overnight. Water was added, and it was extracted with ethyl acetate. The combined organic phases were washed with brine, dried over $MgSO_4$, filtered, and concentrated to dryness. The residue was purified by flash chromatography (SiO_2, DCM/MeOH up to 10%) to give 4-methyl-9-phenethyl-1-oxa-4,9-diazaspiro[5.5]undecan-3-one (**14i** free base) as a yellow oil (291 mg, 86% yield). To a solution of the previous free base (200 mg, 0.69 mmol) in a mixture of diethyl ether (4 mL) and MeOH (0.1 mL), a solution of HCl (0.38 mL, 2 M in diethyl ether, 0.76 mmol) was added under stirring, upon which a solid started to precipitate immediately. The resulting suspension was stirred for 1 h at rt. Then, the solids were collected by filtration, washed with diethyl ether, and dried under vacuum to obtain **14i** HCl salt as a white solid (155 mg, 69% yield). ^{1}H NMR (400 MHz, CD_3OD) δ 7.40−7.22 (m, 5H), 4.17 (s, 2H), 3.61−3.52 (m, 2H), 3.45−3.34 (m, 4H), 3.29−3.20 (m, 2H), 3.15−3.05 (m, 2H), 3.00 (s, 3H), 2.22 (d, J = 13.7 Hz, 2H), 1.99 (t, J = 13.6 Hz, 2H). HPLC−MS: purity 100%. HRMS $[M + H]^+$ (diff ppm) 289.1921 (−3.79).

4-Methyl-9-phenethyl-2-phenyl-1-oxa-4,9-diazaspiro[5.5]-undecan-3-one Hydrochloride (14l) (Representative Example of Scheme 3). To a solution of 4-((methylamino)methyl)-1-phenethylpiperidin-4-ol (**22**, 572 mg, 2.30 mmol) and TEA (0.77 mL, 5.53 mmol) in DCM (27 mL), a solution of 2-chloro-2-phenylacetyl chloride (0.55 mL, 3.45 mmol) in DCM (27 mL) was added dropwise at 0 °C under a nitrogen atmosphere. The reaction mixture was stirred at 0 °C for 2 h. Saturated aqueous $NaHCO_3$ was added, and it was extracted with DCM. The combined organic phases were washed with brine, dried over $MgSO_4$, filtered, and concentrated to dryness to give crude 2-chloro-*N*-((4-hydroxy-1-phenethylpiperidin-4-yl)methyl)-*N*-methyl-2-phenylacetamide as an orange oil (950 mg, overweight, quantitative yield assumed). To a solution of the previous crude compound (950 mg, 923 mg theoretical weight, 2.30 mmol) in dry THF (40 mL), cooled to −78 °C under a nitrogen atmosphere, potassium *tert*-butoxide solution (3.45 mL, 1 M in THF, 3.45 mmol) was slowly added at −78 °C, and then the reaction mixture was allowed to warm and stirred at −30 °C for 4 h. Saturated aqueous NH_4Cl was then added, and it was extracted with ethyl acetate. The combined organic phases were washed with brine, dried over $MgSO_4$, filtered, and concentrated to dryness. The residue was purified by flash chromatography (SiO_2, DCM/MeOH up to 10%) to give 4-methyl-9-phenethyl-2-phenyl-1-oxa-4,9-diazaspiro[5.5]-undecan-3-one (**14l** free base) as an oil (349 mg, 42%). To a solution of the previous free base (150 mg, 0.41 mmol) in diethyl ether (2 mL), a solution of HCl (0.2 mL, 2 M in diethyl ether, 0.41 mmol) was added under stirring, upon which a solid started to precipitate immediately. The resulting suspension was stirred for 2 h at rt. Then, the solids were collected by filtration, washed with diethyl ether, and dried under vacuum to obtain **14l** HCl salt as a white solid (66 mg, 40% yield). ^{1}H NMR (400 MHz, CD_3OD) δ 7.46−7.40 (m, 2H), 7.39−7.23 (m, 8H), 5.18 (s, 1H), 3.83 (d, J = 12.9 Hz, 1H), 3.68−3.61 (m, 1H), 3.59−3.53 (m, 1H), 3.42−3.22 (m, 5H), 3.14−3.07 (m, 2H), 3.03 (s, 3H), 2.59 (d, J = 15.7 Hz, 1H), 2.18−1.94 (m, 3H). HPLC−MS: purity 100%. HRMS $[M + H]^+$ (diff ppm) 365.2221 (0.32)

https://dx.doi.org/10.1021/acs.jmedchem.0c01127
J. Med. Chem. XXXX, XXX, XXX−XXX

2,2,4-Trimethyl-9-phenethyl-1-oxa-4,9-diazaspiro[5.5]-undecan-3-one Hydrochloride (14m) (Representative Example of Scheme 3 Bearing Disubstitution in Position 2). To a solution of 4-((methylamino)methyl)-1-phenethylpiperidin-4-ol (**22**, 496 mg, 2.00 mmol) in DCM (64 mL), $NaHCO_3$ (337 mg, 4.01 mmol) was added at rt. Finally, 2-bromoisobutyryl bromide (0.30 mL, 2.41 mmol) was added dropwise under a nitrogen atmosphere, and the reaction mixture was stirred at rt overnight. 0.1 M K_2CO_3 was added, the phases were separated, and the aqueous phase was back-extracted with DCM. The combined organic phases were dried over $MgSO_4$, filtered, and concentrated to dryness to give crude 2-bromo-*N*-((4-hydroxy-1-phenethylpiperidin-4-yl)methyl)-*N*,2-dimethylpropanamide as a yellow oil (749 mg, 94%). To a solution of the previous crude compound (749 mg, 1.88 mmol) in dry THF (32 mL), cooled to −78 °C under a nitrogen atmosphere, potassium *tert*-butoxide solution (3.77 mL, 1 M in THF, 3.77 mmol) was slowly added at −78 °C, and then the reaction mixture was allowed to warm to 0 °C over a period of 1 h and further stirred at 0 °C for 2 h. Saturated aqueous NH_4Cl was then added, and it was extracted with ethyl acetate. The combined organic phases were dried over $MgSO_4$, filtered, and concentrated to dryness. The residue was purified by flash chromatography (SiO_2, DCM/MeOH up to 10%) to give 2,2,4-trimethyl-9-phenethyl-1-oxa-4,9-diazaspiro[5.5]undecan-3-one (**14m** free base) as an oil (275 mg, 46%). To a solution of the previous free base (275 mg, 0.87 mmol) in diethyl ether (4 mL), a solution of HCl (0.52 mL, 2 M in diethyl ether, 1.04 mmol) was added under stirring, upon which a solid started to precipitate immediately. The resulting suspension was stirred for 1 h at rt. Then, the solids were collected by filtration, washed with diethyl ether, and dried under vacuum to obtain **14m** HCl salt as a white solid (264 mg, 86% yield). ^{1}H NMR (400 MHz, CD_3OD) δ 7.39−7.22 (m, 5H), 3.64−3.55 (m, 2H), 3.49 (s, 2H), 3.44−3.36 (m, 2H), 3.34−3.24 (m, 2H), 3.14−3.06 (m, 2H), 3.03 (s, 3H), 2.10−2.00 (m, 2H), 1.98−1.86 (m, 2H), 1.43 (s, 6H). HPLC−MS: purity 99%. HRMS $[M + H]^+$ (diff ppm) 317.2234 (−3.4).

12-Methyl-8-phenethyl-4-oxa-8,12-diazadispiro[2.1.5.3]-tridecan-13-one Hydrochloride (14n). Step 1: To a solution of *tert*-butyl 1-oxa-6-azaspiro[2.5]octane-6-carboxylate (**6**, 10.00 g, 46.89 mmol) in a mixture of EtOH−water 9:1 (200 mL), 4-methoxybenzylamine (6.43 g, 46.90 mmol) was added. The reaction mixture was heated at 100 °C overnight in a sealed vessel. The solvent was removed under vacuum and the residue was purified by flash chromatography (SiO_2, DCM/MeOH up to 20%) to give *tert*-butyl 4-hydroxy-4-(((4-methoxybenzyl)amino)methyl)piperidine-1-carboxylate (**23**) as a yellow oil (13.55 g, 82%). ^{1}H NMR (400 MHz, $CDCl_3$) δ 7.25−7.20 (m, 2H), 6.89−6.84 (m, 2H), 3.80 (s, 3H), 3.89−3.70 (br s, 2H), 3.78 (s, 2H), 3.15 (t, J = 11.7 Hz, 2H), 2.55 (s, 2H), 1.54−1.47 (m, 2H), 1.45 (s, 9H), 1.43−1.35 (m, 2H). HPLC−MS: purity 98%, m/z = 351.2 $[M + H]^+$.

Step 2: To a solution of compound **23** (9.94 g, 28.36 mmol) and TEA (9.5 mL, 68.16 mmol) in DCM (500 mL), a solution of 2-bromo-4-chlorobutanoyl chloride[19] (9.35 g, 42.53 mmol) in DCM (200 mL) was added dropwise at 0 °C under a nitrogen atmosphere. The reaction mixture was stirred at 0 °C for 2 h. Saturated aqueous $NaHCO_3$ was added, and it was extracted with DCM. The combined organic phases were dried over $MgSO_4$, filtered, and concentrated to dryness to give crude *tert*-butyl 4-((2-bromo-4-chloro-*N*-(4-methoxybenzyl)butanamido)methyl)-4-hydroxypiperidine-1-carboxylate as an orange oil (15.10 g, quantitative). To a solution of the previous crude compound (14.80 g, 27.72 mmol) in THF (185 mL), cooled to 0 °C under a nitrogen atmosphere, potassium *tert*-butoxide solution (111 mL, 1 M in THF, 111.00 mmol) was slowly added, and the reaction mixture was stirred at 0 °C for 2 h. Saturated aqueous NH_4Cl was then added, and it was extracted with ethyl acetate. The organic phases were combined, dried over $MgSO_4$, filtered, and concentrated to dryness. The residue was purified by flash chromatography (SiO_2, DCM/MeOH up to 10%) to give *tert*-butyl 12-(4-methoxybenzyl)-13-oxo-4-oxa-8,12-diazadispiro[2.1.5.3]-tridecane-8-carboxylate (**24**) as a yellow oil (5.51 g, 48%). ^{1}H NMR (400 MHz, $CDCl_3$) δ 7.18 (d, J = 8.6 Hz, 2H), 6.87 (d, J = 8.7 Hz, 2H), 4.54 (s, 2H), 3.81 (s, 3H), 3.63 (br s, 2H), 3.18 (s, 2H), 3.06 (t, J = 11.4 Hz, 2H), 1.86 (d, J = 13.5 Hz, 2H), 1.43 (s, 9H), 1.48−1.34 (m, 4H), 0.98 (q, J = 4.5 Hz, 2H). HPLC−MS: purity 95%, m/z = 417.2 $[M + H]^+$.

Step 3: To a solution of **24** (1.50 g, 3.60 mmol) in DCM (36 mL), trifluoroacetic acid (2.8 mL, 36.34 mmol) was added, and the reaction mixture was stirred at rt for 4 h. The solvent was evaporated to dryness to give 12-(4-methoxybenzyl)-4-oxa-8,12-diazadispiro[2.1.5.3]tridecan-13-one trifluoroacetate (**25** TFA salt) as a viscous yellow oil (2.30 g, 67 wt %, quantitative). The crude product was used in the following step without further purification. ^{1}H NMR (400 MHz, $CDCl_3$) δ 9.31 (br s, 1H), 8.94 (br s, 1H), 7.20−7.16 (m, 2H), 6.92−6.84 (m, 2H), 4.54 (s, 2H), 3.80 (s, 3H), 3.24 (s, 2H), 3.20 (d, J = 12.1 Hz, 2H), 3.11−2.97 (m, 2H), 2.09 (d, J = 14.4 Hz, 2H), 1.75 (td, J = 14.5, 4.3 Hz, 2H), 1.46 (q, J = 4.7 Hz, 2H), 0.97 (q, J = 4.7 Hz, 2H). HPLC−MS: purity 95%, m/z = 371.1 $[M + H]^+$.

Step 4: A mixture of **25** TFA salt (1.50 g, 67 wt %, 3.60 mmol), (2-bromoethyl)benzene (0.59 mL, 4.33 mmol), sodium iodide (0.32 g, 2.17 mmol), and K_2CO_3 (2.49 g, 18.05 mmol) in acetonitrile (36 mL) was heated at 80 °C in a sealed tube overnight. Water was added, and it was extracted with ethyl acetate. The combined organic phases were washed with brine, dried over $MgSO_4$, filtered, and concentrated to dryness. The residue was purified by flash chromatography (SiO_2, DCM/MeOH up to 10%) to give 12-(4-methoxybenzyl)-8-phenethyl-4-oxa-8,12-diazadispiro[2.1.5.3]tridecan-13-one (**26**) as an oil (1.17 g, 77%). ^{1}H NMR (400 MHz, $CDCl_3$) δ 7.30−7.25 (m, 2H), 7.23−7.17 (m, 5H), 6.88−6.84 (m, 2H), 4.55 (s, 2H), 3.80 (s, 3H), 3.19 (s, 2H), 2.80−2.68 (m, 2H), 2.58−2.47 (m, 4H), 2.31 (td, J = 11.4, 2.7 Hz, 2H), 1.97−1.87 (m, 2H), 1.66−1.48 (m, 2H), 1.42 (dd, J = 7.9, 4.5 Hz, 2H), 0.99 (dd, J = 7.9, 4.5 Hz, 2H). HPLC−MS: purity 92%, m/z = 421.1 $[M + H]^+$.

Step 5: A mixture of **26** (0.17 g, 0.40 mmol) and CAN (0.57 g, 1.21 mmol) in a mixture of acetonitrile−water 1:1 (4 mL) was stirred at rt for 7 h. Saturated aqueous Na_2CO_3 was added, and it was extracted with ethyl acetate. The combined organic phases were washed with brine, dried over $MgSO_4$, filtered, and concentrated to dryness. The residue was purified by eluting through an acidic ion-exchange resin cartridge (SCX) to give 8-phenethyl-4-oxa-8,12-diazadispiro[2.1.5.3]-tridecan-13-one (**27**) as a pale brown oil (106 mg, 88%). The crude product was used in the following step without further purification. ^{1}H NMR (400 MHz, $CDCl_3$) δ 7.32−7.27 (m, 2H), 7.23−7.17 (m, 3H), 5.83 (br s, 1H, NH), 3.37 (d, J = 2.7 Hz, 2H), 2.84−2.77 (m, 2H), 2.71−2.57 (m, 4H), 2.39 (t, J = 10.2 Hz, 2H), 2.08−2.00 (m, 2H), 1.79−1.70 (m, 2H), 1.37 (dd, J = 8.0, 4.6 Hz, 2H), 1.02 (q, J = 4.6 Hz, 2H).

Step 6: To a solution of **27** (106 mg, 0.35 mmol) in dry THF (3.5 mL), NaH (16 mg, 60 wt % in mineral oil, 0.39 mmol) was added. The reaction mixture was stirred at rt for 30 min, then iodomethane (0.02 mL, 0.39 mmol) was added, and the resulting mixture was stirred at rt overnight. Saturated aqueous $NaHCO_3$ was added, and it was extracted with DCM. The organic phases were combined, dried over $MgSO_4$, filtered, and concentrated to dryness. The residue was purified by flash chromatography (SiO_2, DCM/MeOH up to 20%) to obtain 12-methyl-8-phenethyl-4-oxa-8,12-diazadispiro[2.1.5.3]-tridecan-13-one (**14n** free base) as a colorless oil (25 mg, 23%). To a solution of the previous free base (25 mg, 0.08 mmol) in anhydrous diethyl ether (0.5 mL), HCl (2 M solution in diethyl ether, 0.04 mL, 0.08 mmol) was added. The mixture was stirred at rt for 1 h and then it was concentrated to dryness to give **14n** HCl salt as a white solid (25 mg, 89%). ^{1}H NMR (400 MHz, CD_3OD) δ 7.38−7.24 (m, 5H), 3.58 (d, J = 11.6 Hz, 2H), 3.50 (s, 2H), 3.42−3.35 (m, 2H), 3.17 (t, J = 12.9 Hz, 2H), 3.11−3.05 (m, 2H), 3.01 (s, 3H), 2.30 (d, J = 14.9 Hz, 2H), 1.97 (t, J = 14.3 Hz, 2H), 1.29 (q, J = 4.6 Hz, 2H), 1.14−1.05 (m, 2H). HPLC−MS: purity 94%. HRMS $[M + H]^+$ (diff ppm) 315.208 (−3.92).

(*R*)-4-Ethyl-2-methyl-9-phenethyl-1-oxa-4,9-diazaspiro-[5.5]undecan-3-one Hydrochloride (14o). Starting from racemic 4-ethyl-2-methyl-9-phenethyl-1-oxa-4,9-diazaspiro[5.5]undecan-3-one (**14e**, 449 mg, prepared following Scheme 1 as described for

https://dx.doi.org/10.1021/acs.jmedchem.0c01127
J. Med. Chem. XXXX, XXX, XXX−XXX

compound **14f**), a chiral preparative HPLC separation (column, CHIRALCEL OJ; temperature, ambient; flow, 16 mL/min; eluent, *n*-heptane/(IPA + 0.33% DEA) 95/5 v/v) was carried out to give (*R*)-4-ethyl-2-methyl-9-phenethyl-1-oxa-4,9-diazaspiro[5.5]undecan-3-one (**14o**) as a colorless oil (161 mg), together with its *S*-enantiomer (138 mg). Absolute configuration was assigned using a sample of compound **14o** obtained via the chiral route displayed in Scheme 4 (exemplified with the preparation of compound **14u**).

To a solution of **14o** free base (161 mg, 0.51 mmol) in anhydrous diethyl ether (2 mL), HCl (2 M solution in diethyl ether, 0.33 mL, 0.66 mmol) was added. The mixture was stirred at rt for 1 h. Then, the solids were collected by filtration, washed with diethyl ether, and dried under vacuum to obtain **14o** HCl salt as a white solid (156 mg, 86%) with ee 98.5% (chiral HPLC). ^{1}H NMR (400 MHz, CD_3OD) δ 7.39−7.25 (m, 5H), 4.23 (q, J = 6.7 Hz, 1H), 3.62−3.52 (m, 3H), 3.51−3.45 (m, 1H), 3.43−3.33 (m, 4H), 3.27 (d, J = 12.8 Hz, 1H), 3.24−3.16 (m, 1H), 3.15−3.08 (m, 2H), 2.39 (dd, J = 15.4, 2.4 Hz, 1H), 2.12−2.02 (m, 1H), 1.97−1.85 (m, 2H), 1.41 (d, J = 6.7 Hz, 3H), 1.15 (t, J = 7.2 Hz, 3H). HPLC−MS: purity 99%. HRMS [M + H]$^+$ (diff ppm) 317.2227 (−1.06).

(*R*)-9-(2,5-Difluorophenethyl)-4-ethyl-2-methyl-1-oxa-4,9-diazaspiro[5.5]undecan-3-one Hydrochloride (14u) (Representative Example of Scheme 4). Step 1: To a solution of *tert*-butyl 1-oxa-6-azaspiro[2.5]octane-6-carboxylate (**6**, 46.10 g, 0.22 mol) in a mixture of EtOH−water 9:1 (745 mL), ethylamine solution (508 mL, 70% solution in water, 4.32 mol) was added, and the reaction mixture was stirred at rt overnight. The solvent was removed under vacuum to give *tert*-butyl 4-hydroxy-4-((ethylamino)methyl)-piperidine-1-carboxylate (**16-1**) as a pale yellow oil (55.90 g, quantitative yield). ^{1}H NMR (400 MHz, $CDCl_3$) δ 3.84 (br s, 2H), 3.16 (t, J = 11.7 Hz, 2H), 2.69 (q, J = 7.1 Hz, 2H), 2.51 (s, 2H), 1.52−1.35 (m, 4H), 1.45 (s, 9H), 1.09 (t, J = 7.1 Hz, 3H). HPLC−MS: purity 100%, m/z= 259.1 [M + H]$^+$.

Step 2: To a solution of **16-1** (55.90 g, 0.22 mol) in ethyl acetate (500 mL), a solution of K_2CO_3 (83.70 g, 0.60 mol) in water (608 mL) was added. After cooling to 0 °C, a solution of (*S*)-2-chloropropanoyl chloride (**8-1S**, 37.33 g, 0.29 mol) in EtOAc (336 mL) was added dropwise over 40 min, maintaining the internal temperature at <5 °C. The reaction mixture was stirred at 0−5 °C for additional 30 min. Then, the layers were separated and the aqueous phase was extracted with ethyl acetate (2 × 300 mL). The organic phases were combined, washed with cold 0.5 M HCl aqueous solution (400 mL), then saturated aqueous $NaHCO_3$ (400 mL), dried over $MgSO_4$, filtered, and concentrated to dryness to give crude (*S*)-*tert*-butyl 4-((2-chloro-*N*-ethylpropanamido)methyl)-4-hydroxypiperidine-1-carboxylate as a white solid (75.70 g, quantitative yield). A solution of the previous crude compound (75.42 g, 0.22 mol) in THF (1.12 L) was cooled to −70 °C using a dry ice/acetone bath. Then, a solution of potassium *tert*-butoxide (238 mL, 1 M in THF, 0.24 mol) was added dropwise over 50 min, maintaining the internal temperature below −60 °C. The reaction mixture was stirred at the same temperature for additional 30 min. NH_4Cl saturated solution (600 mL) was then added, the reaction mixture was warmed to rt, and it was extracted with ethyl acetate (2 × 300 mL). The organic phases were combined, dried over $MgSO_4$, filtered, and concentrated under vacuum to yield crude (*R*)-*tert*-butyl 4-ethyl-2-methyl-3-oxo-1-oxa-4,9-diazaspiro[5.5]undecane-9-carboxylate (**11-1R**) as an off-white solid (62.33 g, 92% yield) with ee 89% (chiral HPLC). The crude product was crystallized from hot isopropyl acetate/heptane to enrich ee %: isopropyl acetate (62 mL, 1 volume) was added to crude **11-1R** (62.33 g), and the mixture was heated to 100 °C until total solution. Heptane (53 mL, 0.85 volumes) was added while hot, and the solution was left to stir at rt for 30 min. Then, the mixture was cooled with an ice−water bath. After seeding, a precipitate was formed and the mixture was stirred for 1 h at 0 °C. Then the solids were collected by filtration, washed with cold isopropyl acetate/heptane mixture 1.2:1 (12 mL), and dried under vacuo to give (*R*)-*tert*-butyl 4-ethyl-2-methyl-3-oxo-1-oxa-4,9-diazaspiro[5.5]undecane-9-carboxylate (**11-1R**) as a white solid (41.30 g, 61% global yield) with ee 98.8% (chiral HPLC: column, Chiralpak ADH; temperature, ambient; flow, 0.5 mL/min; mobile phase, *n*-heptane/EtOH 70/30 v/v.). ^{1}H NMR (400 MHz, $CDCl_3$) δ 4.15 (q, J = 6.8 Hz, 1H), 3.81 (br s, 2H), 3.56−3.45 (m, 1H), 3.38 (d, J = 12.3 Hz, 1H), 3.36−3.19 (m, 2H), 3.04 (t, J = 11.8 Hz, 1H), 2.97 (d, J = 12.2 Hz, 1H), 2.10−2.01 (m, 1H), 1.66−1.49 (m, 2H), 1.46 (s, 9H), 1.43 (d, J = 6.8 Hz, 3H), 1.44−1.37 (m, 1H), 1.12 (t, J = 7.2 Hz, 3H). HPLC−MS: purity 100%, m/z = 313.2 [M + H]$^+$.

Step 3: To a solution of **11-1R** (18.20 g, 58.30 mmol) in DCM (583 mL), trifluoroacetic acid (45 mL, 0.58 mol) was added. The reaction mixture was stirred at rt for 3 h, and then it was evaporated to dryness to give crude (*R*)-4-ethyl-2-methyl-1-oxa-4,9-diazaspiro[5.5]-undecan-3-one trifluoroacetate (**12-1R** TFA salt) as a viscous oil (46.63 g, overweight, estimated 41 wt %; theoretical weight 19.01 g; quantitative yield was assumed) that was used in the following step without further purification. ^{1}H NMR (400 MHz, $CDCl_3$) δ 8.90 (br s, 2H), 4.18 (q, J = 6.7 Hz, 1H), 3.59−3.30 (m, 6H), 3.19−3.07 (m, 2H), 2.30 (dd, J = 15.4, 2.5 Hz, 1H), 2.07−1.95 (m, 1H), 1.94−1.78 (m, 2H), 1.46 (d, J = 6.8 Hz, 3H), 1.15 (t, J = 7.2 Hz, 3H). HPLC−MS: purity 100%, m/z = 213.1 [M + H]$^+$.

Step 4: A mixture of **12-1R** TFA salt (46.63 g, 41 wt %, 58.30 mmol), 2,5-difluorophenethyl methanesulfonate (**13-1**, 22.00 g, 93.20 mmol), and K_2CO_3 (40.30 g, 0.29 mol) in acetonitrile (228 mL) was heated in a sealed vessel at 80 °C overnight. Then, the precipitated solids were filtered off and washed with acetonitrile. The resulting solution was concentrated to dryness. The oily residue was dissolved in methyl *tert*-butyl ether (100 mL), and it was extracted with aqueous 3 M HCl solution (3 × 70 mL). The combined acidic aqueous phases were washed with methyl *tert*-butyl ether (2 × 50 mL) that was discarded, and then basified with aqueous 3 M NaOH solution until pH ∼ 13 and extracted with ethyl acetate (3 × 50 mL). The combined organic phases were dried over $MgSO_4$, filtered, and concentrated to dryness. The crude product was purified by flash chromatography (SiO_2, DCM/MeOH up to 10%) to give (*R*)-9-(2,5-difluorophenethyl)-4-ethyl-2-methyl-1-oxa-4,9-diazaspiro[5.5]-undecan-3-one (**14u** free base) as an oil (14.87 g, 72% yield). To a solution of the previous free base (14.87 g, 42.19 mmol) in a mixture of diethyl ether (300 mL) and MeOH (3.7 mL), a solution of HCl (23.2 mL, 2 M in diethyl ether, 46.40 mmol) was added under stirring, upon which a solid started to precipitate immediately. The resulting suspension was stirred for further 60 min at rt. Then, the solids were collected by filtration, washed with diethyl ether (2 × 7 mL), and dried under vacuum to obtain **14u** HCl salt as a white solid (14.58 g, 89% yield) with ee 99.0% (chiral HPLC). ^{1}H NMR (400 MHz, CD_3OD) δ 7.20−7.12 (m, 2H), 7.11−7.03 (m, 1H), 4.22 (q, J = 6.7 Hz, 1H), 3.59 (d, J = 12.2 Hz, 2H), 3.54 (d, J = 12.9 Hz, 1H), 3.52−3.45 (m, 1H), 3.44−3.33 (m, 4H), 3.28−3.20 (m, 2H), 3.19−3.12 (m, 2H), 2.40 (dd, J = 15.5, 2.3 Hz, 1H), 2.09−1.99 (m, 1H), 1.98−1.80 (m, 2H), 1.41 (d, J = 6.7 Hz, 3H), 1.14 (t, J = 7.2 Hz, 3H). HPLC−MS: purity 99%. HRMS [M + H]$^+$ (diff ppm) 353.2028 (1.61).

12-Ethyl-8-(2-(pyridin-2-yl)ethyl)-4-oxa-8,12-diazadispiro-[2.1.5.3]tridecan-13-one Hydrochloride (14w). Step 1: To a solution of *tert*-butyl 4-hydroxy-4-((ethylamino)methyl)piperidine-1-carboxylate (**16-1**, 11.87 g, 45.94 mmol) in ethyl acetate (119 mL), a solution of K_2CO_3 (17.8 g, 129.00 mmol) in water (83 mL) was added. After cooling to 0−5 °C, a solution of 2-bromo-4-chlorobutanoyl chloride[19] (13.70, 62.50 mmol) in EtOAc (25 mL) was added dropwise, and the reaction mixture was further stirred at 0−5 °C for 1 h. Then, saturated aqueous $NaHCO_3$ was added, the layers were separated, and the aqueous phase was extracted with ethyl acetate. The organic phases were combined, washed twice with cold 0.5 M HCl aqueous solution (70 mL), then saturated aqueous $NaHCO_3$ (70 mL), dried over Na_2SO_4, filtered, and concentrated to dryness to give crude *tert*-butyl 4-((2,4-dichloro-*N*-ethylbutanamido)-methyl)-4-hydroxypiperidine-1-carboxylate as a cream solid (21.35 g, slight overweight, quantitative yield assumed). A solution of the previous crude compound (20.30 g theoretical weight, 45.94 mmol) in THF (767 mL) was cooled to −78 °C using a dry ice/acetone bath under a nitrogen atmosphere. Then, a solution of potassium *tert*-butoxide (69 mL, 1 M in THF, 69 mmol) was added dropwise, and

https://dx.doi.org/10.1021/acs.jmedchem.0c01127
J. Med. Chem. XXXX, XXX, XXX−XXX

the reaction mixture was stirred at −78 °C for 15 min, and then it was warmed up to −30 °C and stirred for further 2 h. NH_4Cl saturated solution was then added, and the reaction mixture was warmed to rt and extracted with ethyl acetate. The organic phases were combined, dried over Na_2SO_4, filtered, and concentrated under vacuum to give crude *tert*-butyl 2-(2-chloroethyl)-4-ethyl-3-oxo-1-oxa-4,9-diazaspiro[5.5]undecane-9-carboxylate as an oil (16.80 g, slight overweight, quantitative yield assumed). A solution of the previous crude compound (16.58 g theoretical weight, 45.94 mmol) in THF (120 mL) was cooled to 0−5 °C under a nitrogen atmosphere. Then, a solution of potassium *tert*-butoxide (115 mL, 1 M in THF, 115 mmol) was added dropwise, and the reaction mixture was stirred at 0−5 °C for 2 h. NH_4Cl saturated solution was then added, and the reaction mixture was warmed to rt and extracted with ethyl acetate. The organic phases were combined, dried over Na_2SO_4, filtered, and concentrated under vacuum to give *tert*-butyl 12-ethyl-13-oxo-4-oxa-8,12-diazadispiro[2.1.5.3]tridecane-8-carboxylate (**28**) as a brown oil (14.90 g, quantitative). ^{1}H NMR (400 MHz, $CDCl_3$) δ 3.79 (s, 2H), 3.45 (q, J = 7.2 Hz, 2H), 3.30 (s, 2H), 3.10 (t, J = 11.2 Hz, 2H), 2.00−1.90 (m, 2H), 1.60−1.49 (m, 2H), 1.46 (s, 9H), 1.36 (dd, J = 7.8, 4.5 Hz, 2H), 1.13 (t, J = 7.2 Hz, 3H), 0.94 (dd, J = 7.8, 4.5 Hz, 2H).. HPLC−MS: purity 100%, m/z = 325.2 $[M + H]^+$.

Step 2: To a solution of **28** (107 mg, 0.33 mmol) in DCM (5 mL), trifluoroacetic acid (0.25 mL, 3.30 mmol) was added, and the reaction mixture was heated at 40 °C for 2 h. The reaction mixture was evaporated to dryness to give crude 12-ethyl-13-oxo-4-oxa-8,12-diazadispiro[2.1.5.3]tridecane trifluoroacetate (**29** TFA salt) as a viscous oil (141 mg, overweight, estimated 79 wt %; theoretical weight 112 mg; quantitative yield was assumed), that was used in the following step without further purification. ^{1}H NMR (400 MHz, CD_3OD) δ 3.49 (s, 2H), 3.46 (q, J = 7.2 Hz, 2H), 3.33−3.27 (m, 1H), 3.20−3.07 (m, 3H), 2.23−2.15 (m, 2H), 1.93−1.83 (m, 2H), 1.29 (dd, J = 8.0, 4.6 Hz, 2H), 1.15 (t, J = 7.2 Hz, 3H), 1.04 (dd, J = 8.0, 4.6 Hz, 2H). HPLC−MS: purity 97%, m/z = 225.1 $[M + H]^+$.

Step 3: A mixture of **29** TFA salt (141 mg, 79 wt %, 0.33 mmol), 2-(2-bromoethyl)pyridine hydrobromide (105 mg, 0.39 mmol), sodium iodide (29 mg, 0.19 mmol), and K_2CO_3 (363 mg, 2.63 mmol) in acetonitrile (5 mL) was heated at 80 °C in a sealed tube overnight. Water was added, and it was extracted with ethyl acetate. The combined organic phases were washed with brine, dried over $MgSO_4$, filtered, and concentrated to dryness. The residue was purified by flash chromatography (SiO_2, DCM/MeOH up to 20%) to give 12-ethyl-8-(2-(pyridin-2-yl)ethyl)-4-oxa-8,12-diazadispiro[2.1.5.3]-tridecan-13-one (**14w** free base) as a yellow oil (72 mg, 66%). To a solution of the previous free base (72 mg, 0.22 mmol) in anhydrous diethyl ether (1 mL), HCl (2 M solution in diethyl ether, 0.11 mL, 0.22 mmol) was added. The mixture was stirred at rt for 1 h and then it was concentrated to dryness to give **14w** HCl salt as a white solid (74.1 mg, 92%). ^{1}H NMR (400 MHz, CD_3OD) δ 8.65 (d, J = 5.3 Hz, 1H), 8.09 (t, J = 7.7 Hz, 1H), 7.64 (d, J = 8.0 Hz, 1H), 7.57 (t, J = 6.4 Hz, 1H), 3.65−3.56 (m, 4H), 3.53 (s, 2H), 3.47 (q, J = 7.2 Hz, 2H), 3.42 (t, J = 7.6 Hz, 2H), 3.29−3.22 (m, 2H), 2.32−2.23 (m, 2H), 2.15−2.03 (m, 2H), 1.30 (dd, J = 7.9, 4.6 Hz, 2H), 1.17 (t, J = 7.2 Hz, 3H), 1.09 (dd, J = 7.9, 4.6 Hz, 2H). HPLC−MS: purity 98%. HRMS $[M + H]^+$ (diff ppm) 330.2174 (0.78).

9-(2-Fluorophenethyl)-2-methyl-1-oxa-4,9-diazaspiro[5.5]-undecan-3-one Hydrochloride (17). To a solution of *tert*-butyl 2-methyl-3-oxo-1-oxa-4,9-diazaspiro[5.5]undecane-9-carboxylate (**9-1**, 100 mg, 0.35 mmol) in DCM (1.0 mL), trifluoroacetic acid (0.27 mL, 3.52 mmol) was added, and the reaction mixture was stirred at rt for 3 h. The reaction mixture was evaporated to dryness to give crude 2-methyl-1-oxa-4,9-diazaspiro[5.5]undecan-3-one trifluoroacetate as a viscous oil (189 mg, overweight, estimated 56 wt %; theoretical weight 105 mg; quantitative yield was assumed). A mixture of the previous trifluoroacetate salt (189 mg, 56 wt %, 0.35 mmol), 1-(2-bromoethyl)-2-fluorobenzene (86 mg, 0.42 mmol), sodium iodide (32 mg, 0.21 mmol), and K_2CO_3 (245 mg, 1.77 mmol) in acetonitrile (3 mL) was heated at 80 °C in a sealed tube overnight. Water was added, and it was extracted with ethyl acetate. The combined organic phases were washed with brine, dried over $MgSO_4$, filtered, and concentrated to dryness. The residue was purified by flash chromatography (SiO_2, DCM/MeOH up to 20%) to give 9-(2-fluorophenethyl)-2-methyl-1-oxa-4,9-diazaspiro[5.5]undecan-3-one (**17** free base) as an oil (53 mg, 49%). To a solution of the previous free base (53 mg, 0.17 mmol) in anhydrous diethyl ether (0.5 mL), HCl (2 M solution in diethyl ether, 0.09 mL, 0.17 mmol) was added. The mixture was stirred at rt for 1 h and then it was evaporated to dryness to give **17** HCl salt as a white solid (45.3 mg, 76%). ^{1}H NMR (400 MHz, CD_3OD) δ 7.39−7.28 (m, 2H), 7.20−7.08 (m, 2H), 4.24 (q, J = 6.8 Hz, 1H), 3.50−3.36 (m, 2H), 3.38 (d, J = 12.7 Hz, 1H), 3.29−3.21 (m, 3H), 3.21 (d, J = 12.7 Hz, 1H), 3.17−3.06 (m, 3H), 2.41 (d, J = 13.1 Hz, 1H), 2.01−1.93 (m, 1H), 1.92−1.80 (m, 2H), 1.42 (d, J = 6.8 Hz, 3H). HPLC−MS: purity 98%. HRMS $[M + H]^+$ (diff ppm) 307.1813 (−0.97).

Single-Crystal X-ray Structure Determination of 14u. *Crystallization and Sample Preparation.* Crystals of the hydrobromide salt of **14u** were obtained by a vapor diffusion experiment of a THF solution of the compound in a heptane atmosphere. The analyzed crystal was prepared for measurement under inert conditions immersed in perfluoropolyether as a protecting oil for manipulation.

Data Collection. Intensity measurements were carried out at the XALOC beamline at the ALBA synchrotron with 13.5 keV radiation (λ = 0.918 44 Å) using a channel-cut Si(111) monochromator and KB mirrors coated with Rh. Data collection was performed using a Bruker (currently Arinax) MD2M diffractometer and the multiaxis MK2 miniKappa goniometer by Arinax. The data were recorded using a Pilatus 2 6M area detector at 295 K. A complete data set was collected using multiple single-axis sweeps at different κ angles. Systematic absences were consistent with chiral space group $P2_1$ (No. 4). Programs used: data collection, in house software Collect; data processing, autoPROC[38] and xia2/DIALS.[39]

Structure Solution and Refinement. The structure was solved by direct methods and refined on F^2 by the full-matrix least-squares method using the programs SHELXS-86 and SHELXL-97.[40] All the H atoms were introduced in calculated positions and refined as riding on their parent atoms with idealized geometries and with restrained isotropic displacement parameters; the H atom bonded to the N2 nitrogen atom was found in difference Fourier maps. Drawing of the structure in Figure 2 was performed with the program Mercury (Cambridge Crystallographic Data Centre, Cambridge, U.K.).[41] Crystal data: $C_{19}H_{27}Br_1F_2N_2O_2$, 433.34 g/mol, monoclinic, $P2_1$, a = 5.896(3) Å, b = 10.936(4) Å, c = 15.917(4) Å, α = 90°, β = 92.152(19)°, γ = 90°, V = 1025.6(7) Å^3, Z = 2, ρ_{calcd} = 1.403 g/cm^3, 9829, measured reflections, 3360 unique reflections, R_{int} = 0.1077, R_1 = 0.0676, wR_2 = 0.1777, Flack parameter[42] = −0.019(8), for 2656 reflections with $I > 2\sigma(I)$, goodness-of-fit = 0.994, highest peak/deepest hole 1.13/−0.38 e/Å^3.

Molecular Simulations of the MOR with Compounds 14u and 14x. Coordinates for the 5C1M structure were downloaded from the opm server[43] to have the system prealigned to the lipid bilayer. All nonligand and nonreceptor molecules except for the nanobody were removed, alternative conformations deleted, side-chains completed for three residues, and acetyl and methylamide capping groups were placed on Met 65 and Phe 347 of the MOR and Gln 3, Val 102, Asp 110,and Ala 127 of the nanobody. The system was typed with CHARMm, residue pK values were calculated, and the protein was ionized at pH 7.4.[44] A binding sphere of 8 Å was defined from the position occupied by BU72 removing the ligand afterward, and the crystallized structure of compound **14u** was docked with Libdock.[45] The obtained complex was exported to Maestro[46] where the chirality of the previous structure was inverted to obtain as well the complex with **14x**. Each system was inserted into a SPC−POPC orthorhombic box with a 10 Å buffer between the system and the edge of the box using the Maestro's system builder. Sodium and chloride ions were added to neutralize and to reach a final concentration of 0.15 M. Both systems were typed with the OPLS force field and equilibrated by an eight-step protocol being the final step a 20 ns NPgT molecular dynamic simulation, where restraints with a force constant of 0.1 were applied to the backbone atoms of the protein.[47] Finally a 500 ns production simulation in the NPgT

https://dx.doi.org/10.1021/acs.jmedchem.0c01127
J. Med. Chem. XXXX, XXX, XXX−XXX

ensemble without any restraints was run for each system and analyzed using Desmond's Simulation Interactions Diagram and Simulation Event Analysis Panel.

Human σ_1 Receptor Radioligand Assay.[21] The binding properties of the test compounds to human σ_1R were studied in transfected HEK-293 membranes using [^{3}H](+)-pentazocine (PerkinElmer, NET-1056) as the radioligand. The assay was carried out with 7 μg of membrane suspension, [^{3}H]-(+)-pentazocine (5 nM, 100 μL) in either absence or presence of either buffer or 10 μM haloperidol for total and nonspecific binding, respectively. Binding buffer contained Tris-HCl (50 mM, at pH 8). Plates were incubated at 37 °C for 120 min. After the incubation period, the reaction mix was transferred to MultiScreen HTS, FC plates (Millipore) were presoaked in 100 μL of 0.1% polyethylenimine and filtered. Then, plates were washed (3 times) with ice-cold Tris-HCl (10 mM, pH 7.4). Filters were dried and counted at approximately 40% efficiency in a MicroBeta scintillation counter (PerkinElmer) using EcoScint liquid scintillation cocktail.

Human μ-Opioid Receptor Radioligand Assay.[2] Transfected CHO-K1 cell membranes (20 μg) were incubated with [^{3}H]-DAMGO (1 nM,) in 250 μL of assay buffer containing 50 mM Tris-HCl and 5 mM $MgCl_2$ at pH 7.4. NBS (nonspecific binding) was measured by adding 10 μM naloxone. The binding of the test compound was measured at five different concentrations. Plates were incubated at 27 °C for 60 min. After the incubation period, the reaction mixture was then transferred to MultiScreen HTS, FC plates (Millipore) presoaked in 100 μL of 0.5% polyethylenimine and filtered. Then, plates were washed 3 times with ice-cold 10 mM Tris-HCl (pH 7.4). Filters were dried and counted at approximately 40% efficiency in a MicroBeta scintillation counter (PerkinElmer) using EcoScint liquid scintillation cocktail.

Human μ-Opioid Receptor Functionality.[22] cAMP measurements on CHO-K1 cells stably expressing human μ-opioid receptor (PerkinElmer, ES-542-C) were performed by using homogeneous time resolved fluorescence (HTRF). 2500 cells/well were seeded the day before the experiment in Opti-Mem (10 μL) in 384-well plates. The compounds were prepared in Opti-Mem with 0.5 mM IBMX and 7.5 μM forskolin, and 10 μL was added to the cells. After 45 min at 37 °C the reaction was stopped by lysing the cells with a mixture of 10 μL of each HTRF detection reagents (Cisbio, 62AM4PEJ). Plates were incubated for an additional 1 h at room temperature and read at 665 nm/620 nm using a RubyStar Plate reader (BMG LabTech).

DAMGO was included in each assay and its maximum effect was considered as E_{max} = 100%.

Human α_1A Adrenoreceptor Radioligand Assay.[2] Human α_1A adrenoreceptor enriched membranes (10 μg) were incubated with 0.2 nM radiolabeled [^{3}H]-prazosin in 250 μL of assay buffer containing 50 mM Hepes, 5 mM $MgCl_2$, 1 mM $CaCl_2$, 0.2% BSA, pH 7.4. NSB (nonspecific binding) was measured by adding 1 μM prazosin in 25 μL volume. Final DMSO concentration was 0.1% (v/v). After 90 min incubation at 25 °C, binding reaction was terminated by filtering 200 μL through Multiscreen GF/C (Millipore) presoaked in 150 μL of 0.5% polyethylenimine in vacuum manifold station, followed by 3 washes with 200 μL/well of ice-cold filtration buffer containing 50 mM Hepes, 500 mM NaCl, BSA 0.1%, pH 7.4.

hERG Assay.[2] CHO cells stably expressing hERG channels (Millipore) were cultured in F12 HAM medium supplemented with 10% FBS and 400 μg/L Geneticin. The extracellular Ringer's solution consisted of the following (in mM): 2 $CaCl_2$, 1 $MgCl_2$, 10 HEPES, 4 KCl, 145 NaCl, 10 glucose, pH 7.4, 305 mOsm. The intracellular Ringer's solution consisted of the following (in mM): 5.37 $CaCl_2$, 1.75 $MgCl_2$, 31.25/10 KOH/EGTA, 10 HEPES, 210 KCl, pH 7.2, 295 mOsm. 4 mM Na_2-ATP was added to intracellular Ringer's solution shortly before use. Whole-cell currents were measured with a QPatch system (Sophion) in response to continuously executed voltage protocols as per manufacturer's recommendations. Upon onset of the voltage protocol, cells were maintained at a holding potential (Vh) of −80 mV, then clamped briefly to −50 mV (20 ms), subsequently depolarized to 20 mV for 4800 ms, and finally repolarized to −50 mV for 5000 ms, at which potential the peak outward tail current was measured. Finally, the voltage returned to Vh for 3100 ms. Thus, voltage protocols were repeated each 15 s. For each cell, extracellular solution was applied previous to increasing concentrations of the tested compound.

In Vivo Studies. Animals. 6- to 8-week-old male CD1 mice were used. All tests were performed in groups of 6−12 animals (n = 6−12). Animals had free access to food and water and were kept in controlled laboratory conditions with temperature at 21 ± 1 °C and a light−dark cycle of 12 h (lights on at 7:00 a.m.). Behavioral testing was conducted in a soundproof and air-regulated experimental room during the light phase and was carried out without knowledge of treatment. All animal husbandry and experimental procedures complied with European guidelines regarding the protection of animals used for experimental and other scientific purposes international standards (European Communities Council directive 2010/63) and were approved by the local ethics committee.

Drug Administration. For systemic administration, compound **14u**, oxycodone, PRE-084, and naloxone were dissolved in a vehicle composed of hydroxypropyl methylcellulose (HPMC) 0.5% in distilled water. The compounds were administered in a volume of 10 mL/kg.

Paw Pressure Test. The test was performed as previously described.[48] Briefly, the animals were gently restrained and a constant pressure (450 g) using a cone-shaped paw-presser with a rounded tip (Analgesy-meter, Ugo-Basile) was applied to the dorsal surface of both hind paws. A chronometer was manually activated at the start of the pressure application and stopped at the onset of the struggle reaction, and the response latency was recorded in seconds. The test was performed once in each hind-paw, with a 1 min interval between each stimulation. A 50 s cutoff was established for each measurement to prevent tissue damage. The mean value of the two measurements was considered in the analyses.

Data were converted to % of antinociception. By comparison with the vehicle mean (defined as 0% of antinociception) and the cutoff (defined as 100% of antinociception), individual percentages of antinociception were determined by the formula % antinociception = [(individual test latency − mean vehicle latency)/(cut-off latency mean vehicle latency)] × 100. Data obtained were compared by using one-way ANOVA. Subsequent post-hoc Sidak's multiple comparison test was used to compare the effects of oxycodone and compound **14u.** Statistical significance criterion was $p < 0.05$.

PSNL Model. (1) Surgery. The partial sciatic nerve ligation model was used to induce neuropathic pain.[49] Briefly, mice were anesthetized with isoflurane (induction, 5%; surgery, 3%), and the common sciatic nerve was exposed at the level of the mid-thigh of the right paw. At about 1 cm proximal to the nerve trifurcation, tight ligation was created around 33−50% of the sciatic nerve, leaving the rest of the nerve uninjured. The muscle was stitched, and the incision was closed with wound clips. The sciatic nerve injury was always produced in the right hind paw (ipsilateral paw), whereas no injury was performed on the left one (contralateral hind paw).

(2) Mechanical Allodynia Assessment. Allodynia to mechanical stimuli was used as outcome measure of neuropathic pain and was quantified by measuring the hind paw withdrawal response to von Frey filament stimulation).[50] Briefly, animals were placed in a Plexiglas box (11 cm × 11 cm × 13 cm) with a wire grid bottom through which the von Frey filaments (bending force range from 0.004 to 2 g) (North Coast Medical, Inc., San Jose CA, USA) were applied by using the up−down paradigm, as previously described. Animals were habituated for 1−2 h before testing in order to allow an appropriate behavioral evaluation. Both ipsilateral and contralateral paws were tested. Clear paw withdrawal, shaking, and licking were considered as nociceptive-like responses.

(3) Opiate Withdrawal Assessment. Opiate withdrawal syndrome was precipitated by injecting naloxone (hydrochloride salt, 1 mg/kg, sc) and evaluating the behavioral responses over 3 consecutive periods of 5 min each (for a total time period of 15 min).[34] Two classes of signs were measured: the number of bouts of jumping, wet dog shakes, paw tremor, and sniffing were counted. On the other hand, teeth chattering, piloerection, salivation, body tremor,

https://dx.doi.org/10.1021/acs.jmedchem.0c01127
J. Med. Chem. XXXX, XXX, XXX−XXX

ptosis, and diarrhea were evaluated with one point being given for the presence of each sign during each period of 5 min. The number of periods showing the sign were then counted (maximum score: 3). A global score was calculated for each animal as the sum of all behavioral responses.

(4) Experimental Protocol. Animals were habituated for 6−7 h to the testing environment during 3−4 days. After the last habituation period, baseline responses were established for von Frey test. One day after baseline measurements, sciatic nerve injury was induced as previously described. In order to verify the appropriate development of neuropathic pain, animals were tested on day 5 after the surgical procedure. The repeated treatment with vehicle, compound **14u**, or oxycodone started on day 13. Mice received the drug twice a day at the dose of 5 mg/kg or 1.25 mg/kg of **14u** or oxycodone respectively, during 10 consecutive days. von Frey evaluations were performed on days 13, 18, and 22 following the same experimental procedure as described before. On day 23, mice received a morning injection vehicle, oxycodone (1.25 mg/kg, ip), or compound **14u** (5 mg/kg, ip) and 30 min later, naloxone (1 mg/kg, sc). Then the opiate-induced withdrawal was evaluated during a period of 15 min. Mechanical allodynia was expressed as pressure (grams) required for the threshold of response in the von Frey filament stimulation model (mean ± SEM). Data obtained were compared in ipsilateral paws by using one-way ANOVA. Subsequent post-hoc DMS test was used to compare the effects of oxycodone and compound **14u** with vehicle in the von Frey model. Results of opiate withdrawal studies were expressed as a global score (mean ± SEM). Student t test was used for comparison with vehicle. Statistical significance criterion was $p < 0.05$.

Intestinal Transit Inhibition (Constipation). Intestinal transit was evaluated by identifying the leading front of an intragastrically administered marker located in the small intestine. A fresh 5% charcoal suspension in distilled water was prepared. Animals were fasted for 3−4 h and then given vehicle (HPMC 0.5%), oxycodone (20 mg/kg, po), or **14u** (40 mg/kg, ip). Then 30 min later, 0.3 mL of the charcoal suspension was administered by oral route using an intragastric probe, mice were sacrificed 30 min later under CO_2 atmosphere saturation, and the entire length of the small intestine was dissected free and removed from pylorus to ileocecal valve. The distance traveled by the charcoal meal and the total length of the intestine were measured in cm. The percentage of the distance traveled by the charcoal meal in relation to the total length of the intestine was calculated. The percentage of intestinal transit versus the total intestine length of each animal, and the percentage of intestinal transit inhibition versus the vehicle-treated group were calculated as % of inhibition = (((% of intestinal transit of each mouse ×100)/mean % of intestinal transit of control group) − 100) × (−1). Data obtained were compared by using one-way ANOVA. Subsequent post-hoc Sidak's multiple comparison test was used to compare the effects of oxycodone and compound **14u**. Statistical significance criterion was $p < 0.05$.

■ ASSOCIATED CONTENT

Supporting Information

The Supporting Information is available free of charge at https://pubs.acs.org/doi/10.1021/acs.jmedchem.0c01127.

Analytical data for all the final compounds and intermediates, optical purity of enantiopure compounds, and experimental methods for affinity measurement in selectivity panel targets(PDF)

Molecular formula strings and some data (CSV)

■ AUTHOR INFORMATION

Corresponding Author

Carmen Almansa − *ESTEVE Pharmaceuticals S.A., 08038 Barcelona, Spain; WELAB, 08028 Barcelona, Spain;* orcid.org/0000-0001-5665-4685; Phone: 0034650697372; Email: calmansa@welab.barcelona

Authors

Mónica García − *ESTEVE Pharmaceuticals S.A., 08038 Barcelona, Spain; WELAB, 08028 Barcelona, Spain*

Marina Virgili − *Enantia, S.L., 08028 Barcelona, Spain*

Mònica Alonso − *Enantia, S.L., 08028 Barcelona, Spain*

Carles Alegret − *Enantia, S.L., 08028 Barcelona, Spain*

Joan Farran − *Enantia, S.L., 08028 Barcelona, Spain*

Begoña Fernández − *ESTEVE Pharmaceuticals S.A., 08038 Barcelona, Spain; WELAB, 08028 Barcelona, Spain*

Magda Bordas − *ESTEVE Pharmaceuticals S.A., 08038 Barcelona, Spain; WELAB, 08028 Barcelona, Spain*

Rosalia Pascual − *ESTEVE Pharmaceuticals S.A., 08038 Barcelona, Spain; WELAB, 08028 Barcelona, Spain;* orcid.org/0000-0002-2535-0272

Javier Burgueño − *ESTEVE Pharmaceuticals S.A., 08038 Barcelona, Spain; WELAB, 08028 Barcelona, Spain*

Alba Vidal-Torres − *ESTEVE Pharmaceuticals S.A., 08038 Barcelona, Spain; WELAB, 08028 Barcelona, Spain*

Antonio R. Fernández de Henestrosa − *ESTEVE Pharmaceuticals S.A., 08038 Barcelona, Spain; WELAB, 08028 Barcelona, Spain*

Eva Ayet − *ESTEVE Pharmaceuticals S.A., 08038 Barcelona, Spain; WELAB, 08028 Barcelona, Spain*

Manuel Merlos − *ESTEVE Pharmaceuticals S.A., 08038 Barcelona, Spain; WELAB, 08028 Barcelona, Spain*

Jose Miguel Vela − *ESTEVE Pharmaceuticals S.A., 08038 Barcelona, Spain; WELAB, 08028 Barcelona, Spain*

Carlos R. Plata-Salamán − *ESTEVE Pharmaceuticals S.A., 08038 Barcelona, Spain*

Complete contact information is available at: https://pubs.acs.org/10.1021/acs.jmedchem.0c01127

Author Contributions

The manuscript was written through contributions of all authors. All authors have given approval to the final version of the manuscript.

Notes

The authors declare no competing financial interest.

CCDC 1979266 contains the supplementary crystallographic data for this paper. These data can be obtained free of charge from The Cambridge Crystallographic Data Centre via www.ccdc.cam.ac.uk/structures.

■ ACKNOWLEDGMENTS

We thank Adriana Port, Raquel Enrech, Inés Álvarez, Pilar Pérez, Xavier Monroy, Marta Pujol, Enrique Hernández, Javier Farre, Raquel Fernández-Reinoso, Sandra Yeste, Mª José Pretel, Georgia Gris, Carmen Segalés, Bertrand Aubel, Alicia Pardo, Ana Paz Marín, and Daniel Zamanillo for their expert contribution to analytical, in vitro, and in vivo studies, Carlos Cendón and Lydia Cárdenas for their expert contribution to the synthesis of the compounds and the resupply batches of compound **14u**, Glòria Ten for the salt screening of **14u** and the single crystal growth experiments, Joan Andreu Morató, Monica Carro, and Edmundo Ortega for their excellent technical assistance, and Carlos Pérez and Eduardo Villarroel for their contribution to compound management. This work was a part of activities in R&D Projects IDI20130943 and IDI20150915 supported by the Spanish Ministerio de Economía y Competitividad (MINECO), through the Centro para el Desarrollo Tecnológico Industrial (CDTI), cofinanced by the European Union through the European Regional

Development Fund (ERDF; Fondo Europeo de Desarrollo Regional, FEDER).

■ ABBREVIATIONS USED

ADME, absorption, distribution, metabolism, and excretion; α_1AR, α_1A adrenoreceptor; CAN, cerium ammonium nitrate; CNS, central nervous system; hERG, human ether-a-go-go-related gene; MOR, μ-opioid receptor; SAR, structure−activity relationship; σ_1R, σ_1 receptor; σ_1R-KO, σ_1 receptor knockout mice; TMSOI, trimethylsulfoxonium iodide

■ REFERENCES

(1) Meldrum, M. L., Ed. Opioids and Pain Relief: A Historical Perspective. *Progress in Pain Research and Management*; IASP Press: Seattle, WA, 2003; Vol 25.

(2) García, M.; Virgili, M.; Alonso, M.; Alegret, C.; Fernández, B.; Port, A.; Pascual, R.; Monroy, X.; Vidal-Torres, A.; Serafini, M. T.; Vela, J. M.; Almansa, C. 4-Aryl-1-oxa-4,9-diazaspiro[5.5]undecane derivatives as new dual μ-opioid receptor agonists and σ_1 receptor antagonists for the treatment of pain. *J. Med. Chem.* **2020**, *63*, 2434−2454.

(3) Dickenson, A. H.; Suzuki, R. Opioids in neuropathic pain: Clues from animal studies. *Eur. J. Pain* **2005**, *9*, 113−116.

(4) Burford, N. T.; Clark, M. J.; Wehrman, T. S.; Gerritz, S. W.; Banks, M.; O'Connell, J.; Traynor, J. R.; Alt, A. Discovery of positive allosteric modulators and silent allosteric modulators of the μ-opioid receptor. *Proc. Natl. Acad. Sci. U. S. A.* **2013**, *110*, 10830−10835.

(5) Jones, M. R.; Viswanath, O.; Peck, J.; Kaye, A. D.; Gill, J. S.; Simopoulos, T. T. A brief history of the opioid epidemic and strategies for pain medicine. *Pain Ther.* **2018**, *7*, 13−21.

(6) Chien, C. C.; Pasternak, G. W. Sigma antagonists potentiate opioid analgesia in rats. *Neurosci. Lett.* **1995**, *190*, 137−139.

(7) Cendán, C. M.; Pujalte, J. M.; Portillo-Salido, E.; Montoliu, L.; Baeyens, J. M. Formalin-induced pain is reduced in sigma(1) receptor knockout mice. *Eur. J. Pharmacol.* **2005**, *511*, 73−74.

(8) Díaz, J. L.; Cuberes, R.; Berrocal, J.; Contijoch, M.; Christmann, U.; Fernández, A.; Port, A.; Holenz, J.; Buschmann, H.; Laggner, C.; Serafini, M. T.; Burgueño, J.; Zamanillo, D.; Merlos, M.; Vela, J. M.; Almansa, C. Synthesis and biological evaluation of the 1-arylpyrazole class of σ_1 receptor antagonists: Identification of 4-{2-[5-methyl-1-(naphtalen-2-yl)-1*H*-pyrazol-3-yloxy]ethyl}morpholine (S1RA, E-52862). *J. Med. Chem.* **2012**, *55*, 8211−8224.

(9) Vidal-Torres, A.; de la Puente, B.; Rocasalbas, M.; Touriño, C.; Bura, S. A.; Fernández-Pastor, B.; Romero, L.; Codony, X.; Zamanillo, D.; Buschmann, H.; Merlos, M.; Baeyens, J. M.; Maldonado, R.; Vela, J. M. Sigma-1 receptor antagonism as opioid adjuvant strategy: Enhancement of opioid antinociception without increasing adverse effects. *Eur. J. Pharmacol.* **2013**, *711*, 63−72.

(10) Zamanillo, D.; Romero, L.; Merlos, M.; Vela, J. M. Sigma 1 receptor: A new therapeutic target for pain. *Eur. J. Pharmacol.* **2013**, *716*, 78−93.

(11) E.U. Clinical Trials Register. An exploratory, randomized, double blind, placebo controlled, parallel groups Phase II clinical trial to evaluate the efficacy and safety of E-52862 (400 mg) by oral route, as part of an analgesic therapy balanced with morphine, followed by an open label extension, in the treatment of post-operative pain due to abdominal hysterectomy Available from www.clinicaltrialsregister.eu/ctr-search/trial/2011-003302-24/results (accessed Jun 3, 2020).

(12) Mao, J.; Gold, M. S.; Backonja, M. Combination drug therapy for chronic pain: a call for more clinical studies. *J. Pain* **2011**, *12*, 157−166.

(13) (a) Morphy, R.; Rankovic, Z. Designed multiple ligands. An emerging drug discovery paradigm. *J. Med. Chem.* **2005**, *48*, 6523−43. (b) Zhou, J.; Jiang, X.; He, S.; Jiang, H.; Feng, F.; Liu, W.; Qu, W.; Sun, H. Rational design of multitarget-directed ligands: Strategies and emerging paradigms. *J. Med. Chem.* **2019**, *62*, 8881−8914.

(14) Almansa, C.; Vela, J. M. Selective sigma-1 receptor antagonists for the treatment of pain. *Future Med. Chem.* **2014**, *6*, 1179−1199.

(15) Diaz, G. J.; Daniell, K.; Leitza, S. T.; Martin, R. L.; Su, Z.; McDermott, J. S.; Cox, B. F.; Gintant, G. A. The [^{3}H]-dofetilide binding assay is a predictive screening tool for hERG blockade and proarrhythmia: Comparison of intact cell and membrane preparations and effects of altering $[K^+]_o$. *J. Pharmacol. Toxicol. Methods* **2004**, *50*, 187−199.

(16) Sánchez-Fernández, C.; Nieto, F. R.; González-Cano, R.; Artacho-Cordón, A.; Romero, L.; Montilla-García, A.; Zamanillo, D.; Baeyens, J. M.; Entrena, J. M.; Cobos, E. J. Potentiation of morphine-induced mechanical antinociception by σ_1 receptor inhibition: role of peripheral σ_1 receptors. *Neuropharmacology* **2013**, *70*, 348−358.

(17) Virgili, M.; Alonso, M.; Alegret, C.; Almansa, C.; García, M. Alkyl Derivatives of 1-Oxa-4,9-diazaspiroundecane Compounds Having Multimodal Activity Against Pain. PCT Int. Appl. WO2015185209A1, 2015.

(18) Elkins, B.; Ennis, D.; Eriksson, T.; Gibson, S.; Gu, E.; Hassall, I.; Hemmerling, M.; Josefsson, B.; Ivanova, S.; Kavitake, S.; Kumar, S. S.; Kumar, V.; Lingesha, S.; Mensonides-Harsema, M.; Merifield, E.; Mo, J.; Pavey, J.; Pimm, A.; Reuberson, J.; Rogers, M.; Schulz, H.; Strandberg, P.; Zhengyu, W.; Cooper, M. Novel Tricyclic Spiropiperidine Compounds, their Synthesis and their Uses as Modulators of Chemokine Receptor Activity. PCT Int. Appl. WO2008010765A1, 2008.

(19) Corey, E. J.; Chaykovsky, M. Dimethyloxosulfonium methylide ($(CH_3)_2SOCH_2$) and dimethylsulfonium methylide ($(CH_3)_2SCH_2$). Formation and application to organic synthesis. *J. Am. Chem. Soc.* **1965**, *87*, 1353−1364.

(20) Abrecht, S. Method for the Preparation of Alpha-bromo-lactam Derivatives. U.S. Patent US6,114,541, 2000.

(21) DeHaven-Hudkins, D. L.; Fleissner, L. C.; Ford-Rice, F. Y. Characterization of the binding of [^{3}H](+)pentazocine to recognition sites in guinea pig brain. *Eur. J. Pharmacol., Mol. Pharmacol. Sect.* **1992**, *227*, 371−378.

(22) Burgueño, J.; Pujol, M.; Monroy, X.; Roche, D.; Varela, M. J.; Merlos, M.; Giraldo, J. A complementary scale of biased agonism for agonists with differing maximal responses. *Sci. Rep.* **2017**, *7*, 15389.

(23) Cobos, E. J.; Baeyens, J. M.; Del Pozo, E. Phenytoin differentially modulates the affinity of agonist and antagonist ligands for sigma 1 receptors of guinea pig brain. *Synapse* **2005**, *55*, 192−195.

(24) (a) Stresser, D. M. High-throughput Screening of Human Cytochrome P450 inhibitors Using Fluorometric Substrates. Methodology for 25 Enzyme/Substrate Pairs. In *Optimization in Drug Discovery. In Vitro Methods*; Yan, Z., Caldwell, G. W., Eds.; Humana Press: Totowa, NJ, 2004; pp 215−230. (b) Yan, Z.; Caldwell, G. W. Evaluation of Cytochrome P450 inhibition in Human Liver Microsomes. In *Optimization in Drug Discovery. In Vitro Methods*; Yan, Z., Caldwell, G. W., Eds.; Humana Press: Totowa, NJ, 2004; pp 231−244. (c) *Drug Interaction Studies—Study Design, Data Analysis, Implications for Dosing and Labeling*; Center for Drug Evaluation and Research (CDER), Food and Drug Administration, September 2006 and February 2012.

(25) (a) Obach, R. S.; Baxter, J. G.; Liston, T. E.; Silber, B. M.; Jones, B. C.; MacIntyre, F.; Rance, D. J.; Wastall, P. The prediction of human pharmacokinetic parameters from preclinical and in vitro metabolism data. *J. Pharmacol. Exp. Ther.* **1997**, *283*, 46−58. (b) Obach, R. S. Prediction of human clearance of twenty-nine drugs from hepatic microsomal intrinsic clearance data: an examination of in vitro half-life approach and nonspecific binding to microsomes. *Drug Metab. Dispos.* **1999**, *27*, 1350−1359.

(26) Putnam, K. P.; Bombick, D. W.; Doolittle, D.J. Evaluation of eight in vitro assays for assessing the cytotoxicity of cigarette smoke condensate. *Toxicol. In Vitro* **2002**, *16*, 599−607.

(27) (a) Maron, D. M.; Ames, B. N. Revised methods for the Salmonella mutagenicity test. *Mutat. Res.* **1983**, *113*, 173−215. (b) Reifferscheid, G.; Heil, J. Validation of the SOS/umu test using test results of 486 chemicals and comparison with the Ames test and carcinogenicity data. *Mutat. Res., Genet. Toxicol. Test.* **1996**, *369*, 129−145.

https://dx.doi.org/10.1021/acs.jmedchem.0c01127
J. Med. Chem. XXXX, XXX, XXX−XXX

(28) Amidon, G. L.; Lennernäs, H.; Shah, V. P.; Crison, J. R. A theoretical basis for a biopharmaceutic drug classification: the correlation of in vitro drug product dissolution and in vivo bioavailability. *Pharm. Res.* **1995**, *12*, 413−420.
(29) Wager, T. T.; Hou, X.; Verhoest, P. R.; Villalobos, A. Moving beyond Rules: The development of a central nervous system multiparameter optimization (CNS MPO) approach to enable alignment of druglike properties. *ACS Chem. Neurosci.* **2010**, *1*, 435−449.
(30) Walker, M. J. K.; Lê, A. D.; Poulos, C. X.; Cappell, H. Role of central versus peripheral opioid receptors in analgesia induced by repeated administration of opioid antagonists. *Psychopharmacology* **1991**, *104*, 164−166.
(31) Mei, J.; Pasternak, G. W. Modulation of brainstem opiate analgesia in the rat by sigma 1 receptors: a microinjection study. *J. Pharmacol. Exp. Ther.* **2007**, *322*, 1278−1285.
(32) Romero, L.; Zamanillo, D.; Nadal, X.; Sánchez-Arroyos, R.; Rivera-Arconada, I.; Dordal, A.; Montero, A.; Muro, A.; Bura, A.; Segalés, C.; Laloya, M.; Hernández, E.; Portillo-Salido, E.; Escriche, M.; Codony, X.; Encina, G.; Burgueño, J.; Merlos, M.; Baeyens, J. M.; Giraldo, J.; López-García, J. A.; Maldonado, R.; Plata-Salamán, C. R.; Vela, J. M. Pharmacological properties of S1RA, a new sigma-1 receptor antagonist that inhibits neuropathic pain and activity-induced spinal sensitization. *Br. J. Pharmacol.* **2012**, *166*, 2289−306.
(33) Huang, W.; Manglik, A.; Venkatakrishnan, A. J.; Laeremans, T.; Feinberg, E. N.; Sanborn, A. L.; Kato, H. E.; Livingston, K. E.; Thorsen, T. S.; Kling, R. C.; Granier, S.; Gmeiner, P.; Husbands, S. M.; Traynor, J. R.; Weis, W. I.; Steyaert, J.; Dror, R. O.; Kobilka, B. K. Structural insights into mu-opioid receptor activation. *Nature* **2015**, *524*, 315−321.
(34) Maldonado, R.; Stinus, L.; Gold, L. H.; Koob, G. F. Role of different brains structures in the expression of the physical morphine withdrawal syndrome. *J. Pharmacol. Exp. Ther.* **1992**, *261*, 669−677.
(35) An exploratory, randomised, double-blind, placebo and active therapy-controlled, Phase I study, to assess the safety, tolerability, pharmacokinetics, pharmacodynamics, and food- effect of single and multiple ascending oral doses of EST73502 in healthy adults and patients with chronic, moderate moderate-to to-severe osteoarthritis pain. Study EudraCT Number 2018-000258-23.
(36) Baell, J. B.; Holloway, G. A. New substructure filters for removal of Pan Assay Interference Compounds (PAINS) from screening libraries and their exclusion in bioassays. *J. Med. Chem.* **2010**, *53*, 2719−2740.
(37) Box, K. J.; Comer, E. A. Using measured pKa, logP and solubility to investigate supersaturation and predict BCS class. *Curr. Drug Metab.* **2008**, *9*, 869−878.
(38) Vonrhein, C.; Flensburg, C.; Keller, P.; Sharff, A.; Smart, O.; Paciorek, W.; Womack, T.; Bricogne, G. Data processing and analysis with the autoPROC toolbox. *Acta Crystallogr., Sect. D: Biol. Crystallogr.* **2011**, *D67*, 293−302.
(39) Winter, G.; Lobley, C. M. C.; Prince, S. M. Decision making in *xia*2. *Acta Crystallogr., Sect. D: Biol. Crystallogr.* **2013**, *D69*, 1260−1273.
(40) Sheldrick, G. M. A short history of *SHELX*. *Acta Crystallogr., Sect. A: Found. Crystallogr.* **2008**, *A64*, 112−122.
(41) Macrae, C. F.; Bruno, I. J.; Chisholm, J. A.; Edgington, P. R.; McCabe, P.; Pidcock, E.; Rodriguez-Monge, L.; Taylor, R.; van de Streek, J.; Wood, P. A. Mercury CSD 2.0 - new features for the visualization and investigation of crystal structures. *J. Appl. Crystallogr.* **2008**, *41*, 466−470.
(42) Flack, H. D. On enantiomorph-polarity estimation. *Acta Crystallogr., Sect. A: Found. Crystallogr.* **1983**, *A39*, 876−881.
(43) Lomize, A. L.; Pogozheva, I. D.; Lomize, M. A.; Mosberg, H. I. Positioning of proteins in membranes: A computational approach. *Protein Sci.* **2006**, *15*, 1318−1333.
(44) *Discovery Studio 16*; Dassault Systèmes BIOVIA: San Diego, CA, 2016.
(45) Diller, D. J.; Merz, K. M. High throughput docking for library design and library prioritization. *Proteins: Struct., Funct., Genet.* **2001**, *43*, 113−124.
(46) *Schrödinger Release 2017-4: Maestro*; Schrödinger, LLC,: New York, NY, 2020.
(47) Bowers, K. J.; Chow, E.; Xu, H.; Dror, R. O.; Eastwood, M. P.; Gregersen, B. A.; Klepeis, J. L.; Kolossvary, I.; Moraes, M. A.; Sacerdoti, F. D.; Salmon, J. K.; Shan, Y.; Shaw, D. E. Scalable Algorithms for Molecular Dynamics Simulations on Commodity Clusters. *Proceedings of the ACM/IEEE Conference on Supercomputing (SC06)*, Tampa, FL, November 11−17, 2006; ACM/IEEE, 2006.
(48) Randall, L. O.; Selitto, J. J. A method for measurement of analgesic activity on inflamed tissue. *Arch. Int. Pharmacodyn. Ther.* **1957**, *111*, 409−419.
(49) Malmberg, A. B.; Basbaum, A. I. Partial sciatic nerve injury in the mouse as a model of neuropathic pain: behavioral and neuroanatomical correlates. *Pain* **1998**, *76*, 215−222.
(50) Chaplan, S. R.; Bach, F. W.; Pogrel, J. W.; Chung, J. M.; Yaksh, T. L. Quantitative assessment of tactile allodynia in the rat paw. *J. Neurosci. Methods* **1994**, *53*, 55−63.

https://dx.doi.org/10.1021/acs.jmedchem.0c01127
J. Med. Chem. XXXX, XXX, XXX−XXX